Populus euphratica APYRASE2 Enhances Cold Tolerance by Modulating Vesicular Trafficking and Extracellular ATP in Arabidopsis Plants[1][OPEN]

Shurong Deng[2], Jian Sun[2], Rui Zhao[2], Mingquan Ding[2], Yinan Zhang[2], Yuanling Sun, Wei Wang, Yeqing Tan, Dandan Liu, Xujun Ma, Peichen Hou, Meijuan Wang, Cunfu Lu, Xin Shen, and Shaoliang Chen*

College of Biological Sciences and Technology, Beijing Forestry University, Beijing 100083, People's Republic of China (S.D., R.Z., Y.Z., Y.S., W.W., Y.T., D.L., X.M., M.W., C.L., X.S., S.C.); College of Life Science, Jiangsu Normal University, Xuzhou 221116, People's Republic of China (J.S.); College of Agricultural and Food Science, Zhejiang Agricultural and Forestry University, Hangzhou 311300, People's Republic of China (M.D.); and National Engineering Research Center for Information Technology in Agriculture, Beijing 100097, People's Republic of China (P.H.)

ORCID ID: 0000-0002-0835-6963 (M.D.); 0000-0001-7511-3067 (S.C.).

Apyrase and extracellular ATP play crucial roles in mediating plant growth and defense responses. In the cold-tolerant poplar, *Populus euphratica*, low temperatures up-regulate APYRASE2 (PeAPY2) expression in callus cells. We investigated the biochemical characteristics of PeAPY2 and its role in cold tolerance. We found that PeAPY2 predominantly localized to the plasma membrane, but punctate signals also appeared in the endoplasmic reticulum and Golgi apparatus. PeAPY2 exhibited broad substrate specificity, but it most efficiently hydrolyzed purine nucleotides, particularly ATP. PeAPY2 preferred Mg^{2+} as a cofactor, and it was insensitive to various, specific ATPase inhibitors. When *PeAPY2* was ectopically expressed in Arabidopsis (*Arabidopsis thaliana*), cold tolerance was enhanced, based on root growth measurements and survival rates. Moreover, under cold stress, *PeAPY2*-transgenic plants maintained plasma membrane integrity and showed reduced cold-elicited electrolyte leakage compared with wild-type plants. These responses probably resulted from efficient plasma membrane repair via vesicular trafficking. Indeed, transgenic plants showed accelerated endocytosis and exocytosis during cold stress and recovery. We found that low doses of extracellular ATP accelerated vesicular trafficking, but high extracellular ATP inhibited trafficking and reduced cell viability. Cold stress caused significant increases in root medium extracellular ATP. However, under these conditions, *PeAPY2*-transgenic lines showed greater control of extracellular ATP levels than wild-type plants. We conclude that Arabidopsis plants that overexpressed *PeAPY2* could increase membrane repair by accelerating vesicular trafficking and hydrolyzing extracellular ATP to avoid excessive, cold-elicited ATP accumulation in the root medium and, thus, reduced ATP-induced inhibition of vesicular trafficking.

[1] This work was supported by the National Natural Science Foundation of China (grant nos. 31270654, 31200207, and 31200470), the Research Project of the Chinese Ministry of Education (grant no. 113013A), the Key Project for Overseas Scholars by the Ministry of Human Resources and Social Security of the People's Republic of China (grant no. 2012001), the Program of Introducing Talents of Discipline to Universities (111 Project; grant no. B13007), and the Program for Changjiang Scholars and Innovative Research Teams in the University (grant no. IRT13047).

[2] These authors contributed equally to the article.

* Address correspondence to lschen@bjfu.edu.cn.

The author responsible for distribution of materials integral to the findings presented in this article in accordance with the policy described in the Instructions for Authors (www.plantphysiol.org) is: Shaoliang Chen (lschen@bjfu.edu.cn).

S.D., J.S., M.D., and S.C. conceived the original screening and research plans; R.Z., X.S., and C.S. supervised the experiments; S.D., Y.Z., Y.S., W.W., Y.T., D.L., X.M., P.H., and M.W. performed most of the experiments; R.Z., C.L., and X.S. provided technical assistance to S.D.; S.D. designed the experiments, analyzed the data, conceived the project, and wrote the article with contributions of all the authors; S.C. supervised and complemented the writing.

[OPEN] Articles can be viewed without a subscription.

www.plantphysiol.org/cgi/doi/10.1104/pp.15.00581

Low temperature is a major environmental factor that restrains plant growth and crop productivity (Yamaguchi-Shinozaki and Shinozaki, 2006). When temperatures fall below 0°C, plant cells experience dehydration and mechanical injury caused by ice crystallization (Webb and Steponkus, 1993; Yamazaki et al., 2008). Cold stress reduces plasma membrane (PM) integrity, which leads to the leakage of intracellular solutes. ATP can be an important signaling molecule when released into the extracellular matrix (ECM). Extracellular ATP (eATP) was shown to regulate a wide range of cellular processes (Roux and Steinebrunner, 2007; Clark and Roux, 2009, 2011; Tanaka et al., 2010; Clark et al., 2014), but its functions are dose dependent. For example, in Arabidopsis (*Arabidopsis thaliana*), low concentrations of eATP triggered stomatal opening, but high concentrations caused stomatal closure (Clark et al., 2011). Application of eATP at 100 to 200 μM increased hypocotyl elongation in etiolated seedlings, but higher doses led to a reduction of hypocotyl elongation (Roux et al., 2006). In fibers of cotton (*Gossypium hirsutum*), application of

ATPγS and ADPβS at 30 μM each induced an increase in average fiber length, whereas 150 μM ATPγS or ADPβS inhibited the growth of fibers (Clark et al., 2010a). In addition, low doses of eATP (less than 100 μM) induced an obvious Ca^{2+} influx into the elongation zone of Arabidopsis roots, and higher doses of eATP (1,000 μM) caused a significant increase in Ca^{2+} efflux (Demidchik et al., 2011). In *Populus euphratica*, exposure to high levels of ATP (more than 500 μM) was shown to trigger programmed cell death in callus cells, but at low doses (less than 200 μM), callus cells did not die over the observation period (Sun et al., 2012a). The cold-elicited release of ATP through disrupted membranes and the buildup of ATP in the ECM may cause a reduction in cell viability. eATP also plays a fundamental role in mediating plant responses to environmental stresses, such as pathogens (Chivasa et al., 2009), wounds (Cao et al., 2014), high salt (Sun et al., 2012b), and osmotic stress (Jeter et al., 2004; Kim et al., 2009); however, the link between eATP and cold tolerance has not been fully established.

Extracellular apyrases (or ectoapyrases) are the principal enzymes that limit eATP accumulation in both animals and plants (Todorov et al., 1997; Marcus et al., 2003; Wu et al., 2007). In Arabidopsis, suppression of apyrases (AtAPY1 and AtAPY2) led to a slight increase in eATP levels, indicating that APY1 and APY2 controlled the concentration of eATP (Lim et al., 2014). Apyrases are suggested to be involved in some of the signaling steps in plant growth. Apyrases play a crucial role in pollen germination (Steinebrunner et al., 2003; Wu et al., 2007), cotton fiber elongation (Clark et al., 2010a), and root hair growth (Liu et al., 2012). In addition, ectoapyrases contribute to regulating stomatal functions; chemical and immunological inhibition of apyrase activity induced stomatal closure (Clark et al., 2011). Recently, apyrases were shown to play important roles in the signaling steps in plant defense responses (Lim et al., 2014). Suppression of apyrase significantly altered the expression of genes involved in biotic stress responses (Lim et al., 2014). Additionally, our previous finding suggested that apyrase contributed to salt tolerance in *P. euphratica* (Sun et al., 2012b). NaCl shock elicited a significant rise in ATP in the ECM, but the eATP levels returned to basal levels after 20 min of salt treatment (Sun et al., 2012b). This was presumably due to ATP hydrolysis by ectoapyrase, which enabled *P. euphratica* to maintain low levels of eATP in a prolonged duration of salinity and, thus, prevent eATP-induced cell death (Sun et al., 2012a). Apyrase was also postulated to serve as a signal in stress responses. However, no studies have investigated in higher order plants whether apyrase promotes the hydrolysis of ATP at low temperatures and whether this activity is correlated to cold tolerance.

In general, in higher order plants, low temperature causes a reduction in PM integrity. It is necessary for plant cells to reseal the PM disruption to prevent a decrease in cell viability (Yamazaki et al., 2008, 2010). PM resealing requires vesicular trafficking that includes both endocytosis and exocytosis (Togo et al., 1999; McNeil et al., 2003; Tam et al., 2010; Los et al., 2011). Ca^{2+}-dependent exocytosis provides a membrane patch to the wound site, which relieves PM tension for resealing (Togo et al., 2000; Sonnemann and Bement, 2011). In animals, lysosomes are the major organelles that contribute to exocytosis-mediated membrane repair (Gerasimenko et al., 2001; Reddy et al., 2001; McNeil, 2002). Endocytosis also contributes to membrane repair by retrieving the wound site from the PM in a Ca^{2+}-dependent manner (Idone et al., 2008). Shibasaki et al. (2009) suggested that low temperature inhibited the intracellular trafficking of auxin efflux carriers after the initiation of cold stress (9–12 h). However, it remains unclear whether vesicular trafficking is mediated by apyrase and eATP and contributes to cold tolerance during long-term cold stress and the subsequent recovery period.

This study evaluated the roles of apyrase and eATP in cold stress signaling in woody plants. We focused on *P. euphratica*, because this species plays very important roles in stabilizing sand dunes and in sheltering agricultural regions in northwest China (Wei, 1993). In addition, *P. euphratica* trees can adapt to harsh temperature conditions in saline and alkaline desert sites (Wei, 1993). In this study, we showed that cold stress up-regulated *APY2* expression in *P. euphratica* callus cells, but it did not induce the expression of *APY1*, another apyrase (Supplemental Fig. S1). Thus, APY2 may contribute to cold adaptation in *P. euphratica*. We tested this hypothesis by cloning the *PeAPY2* gene from *P. euphratica* callus cells and transferring it into a model species, Arabidopsis. We then investigated the roles of PeAPY2 in eATP control and cold tolerance. Our data showed that *PeAPY2* overexpression increased root membrane integrity and cold tolerance. This was likely due to effective PM repair, because endocytosis and exocytosis were up-regulated in transgenic plants. We concluded that PeAPY2 modulated eATP levels and enhanced vesicular trafficking and that these activities may have contributed to membrane resealing in cold-stressed *PeAPY2*-transgenic plants.

RESULTS

PeAPY2 Expression and eATP Levels in *P. euphratica* Cells under Cold Treatment

In *P. euphratica* cells, [eATP] steadily increased upon the cold treatment (4°C; Fig. 1A). This was due to the increased electrolyte leakage caused by membrane oxidation, because malondialdehyde content, an indicator of lipid peroxidation (Wang et al., 2007, 2008), markedly increased after the initiation of cold stress (Fig. 1A). The slope of [eATP] increase was lowered after day 4, as compared with the first 3 to 4 d of cold stress (Fig. 1A). This was presumably the result of ATP hydrolysis by apyrases, the principal enzymes that hydrolyze eATP in plants (Wu et al., 2007; Tanaka et al., 2011). In accordance, quantitative real-time (qRT)-PCR results showed that cold treatment induced *PeAPY2* expression in *P. euphratica* callus cells. By comparison with the control,

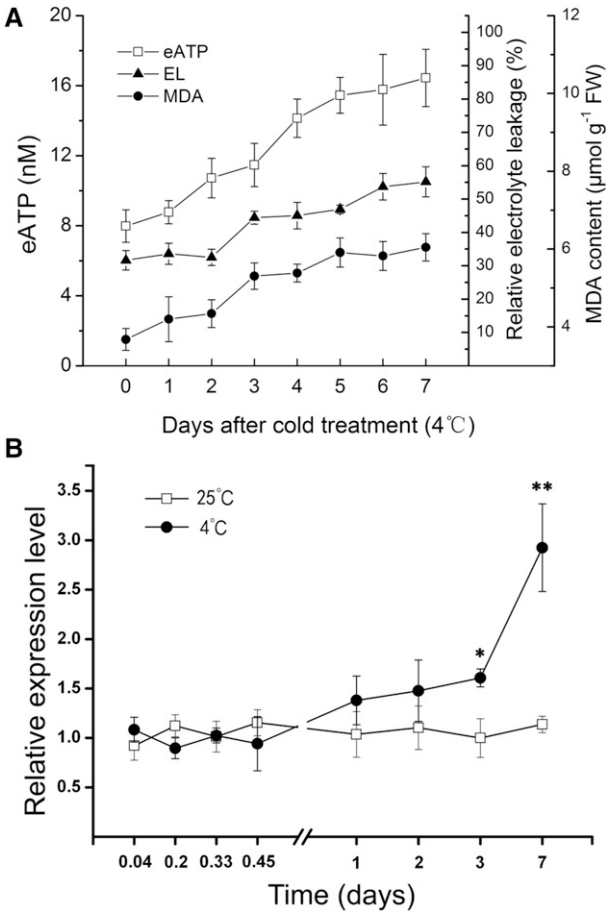

Figure 1. Effects of cold stress on eATP, electrolyte leakage (EL), malondialdehyde (MDA) content, and expression profiles of *PeAPY2* in *P. euphratica* callus cells. *P. euphratica* cells were subjected to 4°C for low-temperature treatment, while control cells were cultured under normal growth conditions at 25°C. A, eATP, electrolyte leakage, and malondialdehyde under cold stress. Cold-stressed and control cells were daily sampled during the period of cold stress. FW, Fresh weight. B, *PeAPY2* mRNA levels during cold stress. Cold-stressed and control cells were sampled after 0, 1, 5, 8, 11, 24, 48, 72, and 168 h of treatment. The expression levels of *PeAPY2* were normalized to the expression level of the *P. euphratica β-ACTIN7* gene (*PeACT7*; internal control) to derive relative expression. Primers designed to target *PeAPY2* and *PeACT7* genes are shown in Supplemental Table S3. Each point is the mean of three independent experiments, and error bars represent SE. *, $P < 0.05$, **, $P < 0.01$, control versus cold treatment.

a slight but not significant increase in *PeAPY2* transcript was observed after 1 d of cold stress (Fig. 1B). Thereafter, *PeAPY2* transcription gradually increased to significant levels after 3 d of cold treatment (4°C); then, transcription increased sharply and peaked on day 7 of cold treatment (Fig. 1B).

Subcellular Localization of PeAPY2

Enhanced yellow fluorescent protein (eYFP) was used to investigate the subcellular localization of PeAPY2 in onion (*Allium cepa*) and Arabidopsis (Fig. 2A). The *PeAPY2-eYFP* fusion construct was transiently expressed in onion with particle bombardment. In nonplasmolyzed onion epidermal cells, the PeAPY2-eYFP fusion protein was present in the cell wall, PM, and cytoplasm (Fig. 2B). When cells were plasmolyzed by exposure to osmotic

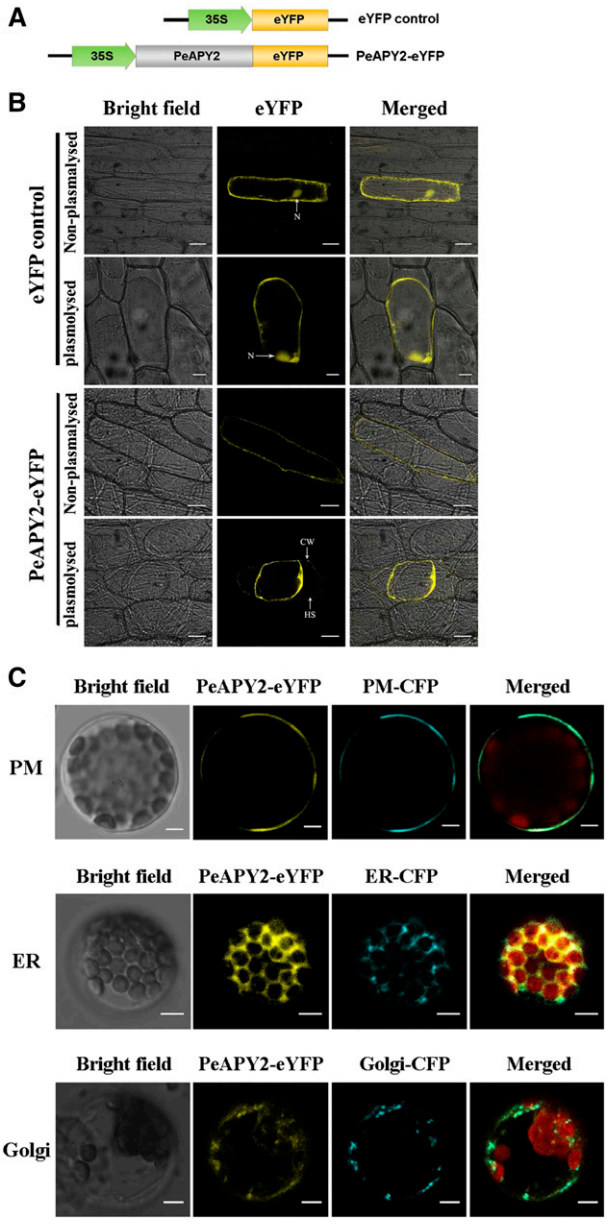

Figure 2. Subcellular localization of PeAPY2 after transient transformation in onion epidermal cells and Arabidopsis mesophyll protoplasts. A, Diagrams of the *eYFP* control (top) and *PeAPY2-eYFP* fusion (bottom) constructs for transformation. B, Representative images of PeAPY2-eYFP transgenic onion cells and eYFP controls. Plasmolysis was induced by hyperosmotic shock with 500 mM NaCl. CW, Cell wall; HS, Hechtian strands; N, nucleus. Bars = 50 μm. C, Representative images show the colocalization (yellow-green in merged images) of PeAPY2-eYFP (yellow) and CFP-tagged (cyan) organelle markers for the PM (PM-CFP; Arabidopsis Biological Resource Center [ABRC] stock no. CD3-1001), ER (ER-CFP; ABRC stock no. CD3-953), and Golgi apparatus (Golgi-CFP; ABRC stock no. CD3-961) in Arabidopsis mesophyll protoplasts. Bars = 5 μm.

shock (0.5 M NaCl), the PeAPY2-eYFP fusion protein remained in the retracted cytoplasm and Hechtian strands connected to the cell wall and PM (Fig. 2B, bottom). Cells transformed with eYFP alone showed yellow fluorescence throughout the cytoplasm and nuclear region in nonplasmolyzed and plasmolyzed cells (Fig. 2B, top).

To localize PeAPY2 in organelles, eYFP-tagged PeAPY2 and organelle markers tagged with cyan fluorescent protein (CFP) were cotransformed into Arabidopsis mesophyll protoplasts (Fig. 2C). Organelle markers were constructed by fusing an N-terminal CFP tag to different proteins that were specifically expressed in the PM, endoplasmic reticulum (ER), and Golgi apparatus. We found that PeAPY2 was colocalized predominantly with the PM marker Arabidopsis Plasma Membrane Intrinsic Protein 2A (AtPIP2A) (Fig. 2C); thus, PeAPY2 was predominantly localized to the PM. We also noticed that PeAPY2-eYFP was partially colocalized with the ER and Golgi makers, showing punctate structures in the cytosol (Fig. 2C). These findings suggested that PeAYP2 is likely produced in the ER and transported through the Golgi to the PM.

Characterization of PeAPY2 Apyrase Activity

Phylogenetic and sequence analyses indicated that PeAPY2 was homologous to apyrases expressed in various plant species (Supplemental Figs. S2 and S3). In this study, the PeAPY2 sequence was tagged with GLUTATHIONE-*S*-TRANSFERASE (GST) and expressed in *Escherichia coli*, and the recombinant protein was purified. To ensure that the recombinant protein resembled the native PeAPY2, we investigated its enzymatic characteristics, including its substrate specificity, sensitivity to ATPase inhibitors, and cofactor preference.

PeAPY2 Substrate Specificity for Hydrolysis of Different Nucleotides

To examine the substrate specificity of purified PeAPY2, we tested a variety of triphosphate or diphosphate nucleotides (Fig. 3A) and measured inorganic phosphate (Pi) release. The ATP-hydrolyzing activity was 75 ± 9.4 μmol Pi h^{-1} mg^{-1} purified PeAPY2 protein (K_m = 390 ± 12 μM, V_{max} = 70.8 ± 9.4 μmol h^{-1} mg^{-1}; Supplemental Fig. S4), which was significantly higher than its activities on other nucleotide substrates (Fig. 3A). Moreover, the enzymatic activity was relatively high over a pH range of 6 to 8 (Supplemental Fig. S5A). Compared with the ATP substrate, PeAPY2 had moderate affinity for GTP, with an activity of 58 ± 11.1 μmol Pi h^{-1} mg^{-1} protein (Fig. 3A). The enzyme also showed some hydrolysis activity for pyrimidine nucleotides, including CTP and UTP, but the activity was 42% to 56% lower than that for ATP and GTP (Fig. 3A). The hydrolysis of ADP and UDP was also less than half of that for ATP. PeAPY2 activity was nearly undetectable for AMP (Fig. 3A), which was similar to observations for other apyrases in plant and animal species (Wang and Guidotti, 1996; Tanaka et al., 2011).

PeAPY2 Insensitivity to Specific Inhibitors of P-, V-, and F-Type ATPases

In general, apyrases are insensitive to specific inhibitors of P-, V-, and F-type ATPases and various types of phosphatases (Steinebrunner et al., 2000). With ATP as substrate, we examined the sensitivity of PeAPY2 to a variety of ATPase inhibitors. We tested NaF, an inhibitor of pyrophosphatase; NaN_3, an inhibitor of F-type ATPases; $NaNO_3$, an inhibitor of V-type ATPases; Na_3VO_4, an inhibitor of P-type ATPases; Na_2MoO_4, an inhibitor of acid phosphatases; and *N*-(3-methylphenyl)-[1,1-biphenyl]-4-sulfonamide (NGXT191), an inhibitor of apyrases isolated from Arabidopsis and potato (*Solanum tuberosum*). The ATP hydrolysis activity of PeAPY2 was not significantly suppressed by any of the tested inhibitors, except NaN_3, which suppressed activity by approximately 25% (5 mM NaN_3; Fig. 3B). The NaN_3 inhibition of PeAPY2 was dose dependent, and its inhibitory effect markedly declined at 1 mM compared with the higher doses of 5 and 10 mM (Supplemental Fig. S5B). Unexpectedly, NGXT191, a strong inhibitor of apyrase activity in Arabidopsis and potato (Windsor et al., 2003; Wu et al., 2007), did not significantly inhibit PeAPY2 (Fig. 3B). This finding implied that there are species differences in apyrase sensitivity to NGXT191 (Tanaka et al., 2011).

PeAPY2 Dependence on Divalent Cations

Apyrase family members require divalent metal ions as cofactors for enzymatic activity (Tanaka et al., 2011). To determine cofactor preference, PeAPY2 activity was assayed in the presence of Mg^{2+}, Ca^{2+}, Zn^{2+}, Cd^{2+}, Mn^{2+}, Co^{2+}, Cu^{2+}, or Ni^{2+}. The results showed that the ATP-hydrolyzing activity of PeAPY2 was enhanced with all the cations tested, except Ni^{2+} (Fig. 3C). The order of preference was as follows: $Mg^{2+} > Ca^{2+} \sim Zn^{2+} \sim Cd^{2+} \sim Mn^{2+} > Co^{2+} > Cu^{2+} \sim Ni^{2+}$ (Fig. 3C). Of note, Ca^{2+} and Mg^{2+} exhibited an additive effect in enhancing PeAPY2 apyrase activity (Fig. 3C). Moreover, both Ca^{2+} and Mg^{2+} enhancements of PeAPY2 activities were significantly reduced by EDTA, a chelator of divalent cations (Fig. 3C).

PeAPY2 Overexpression Enhanced Cold Tolerance and Recovery

Based on our finding that *PeAPY2* was cold inducible in *P. euphratica* cells (Fig. 1), we investigated the role of PeAPY2 in cold tolerance. We performed heterologous overexpression by constitutively expressing *PeAPY2* in Arabidopsis Columbia-0. We obtained six independent, homozygous, overexpression (OE) lines (Fig. 4A). Two transgenic lines, *PeAPY2-OE2* and *PeAPY2-OE4*, showed relatively high expression levels (Fig. 4A); thus, these were selected for cold treatment tests. The third generation of transgenic lines grown on one-half-strength Murashige and Skoog (MS) medium were not significantly different in phenotype from wild-type seedlings and vector controls under control conditions

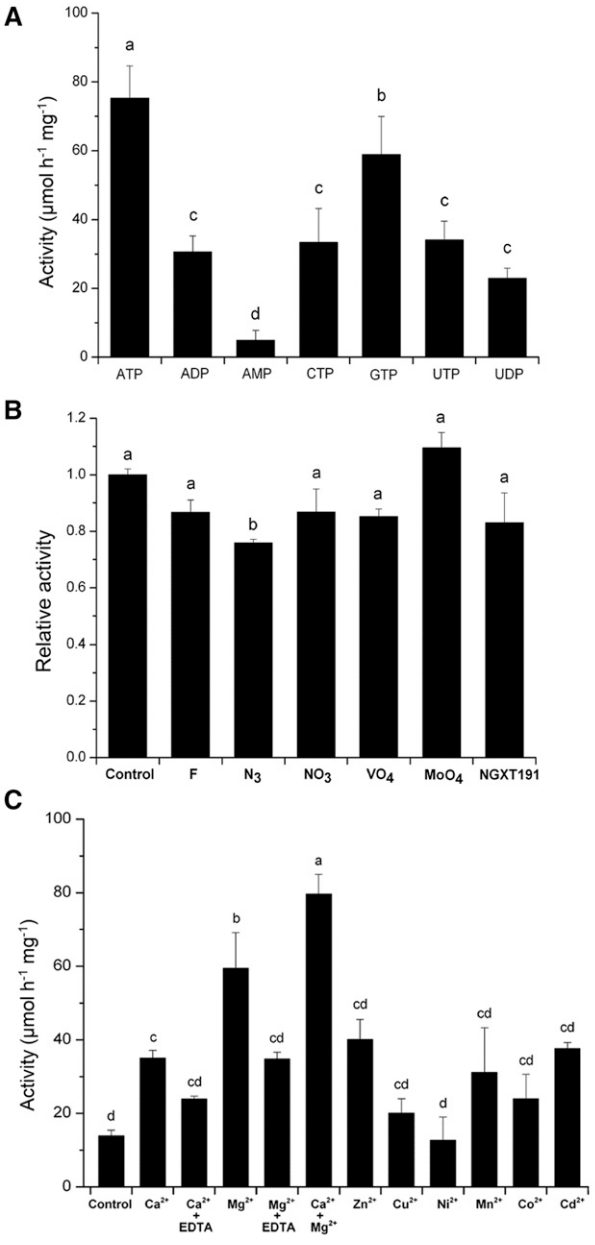

Figure 3. Enzymatic characterization of PeAPY2 recombinant protein. A, Substrate specificity of PeAPY2. Nucleotide triphosphates (ATP, GTP, CTP, and UTP), nucleotide diphosphates (ADP and UDP), and AMP nucleotides (AMP) were applied at a concentration of 3 mM. B, Sensitivity of PeAPY2 to specific inhibitors of various ATPases. The ATPase inhibitors were applied at different concentrations: NaF (fluoride, an inhibitor of pyrophosphatases; 40 mM), NaN_3 (N_3, an inhibitor of F-type ATPases; 5 mM), $NaNO_3$ (NO_3, an inhibitor of V-type ATPases; 50 mM), Na_3VO_4 (VO_4, an inhibitor of P-type ATPases; 1 mM), $NaMoO_4$ (molybdate, an inhibitor of acid phosphatases; 1 mM), and NGXT191 (an inhibitor of apyrases from Arabidopsis and potato; 5 μg mL^{-1}). PeAPY2 activities are expressed relative to the control activity in the absence of inhibitors. C, Effects of different divalent metal ions on PeAPY2 apyrase activity. Apyrase activity was measured in the absence (control) and presence of divalent metal ions (Mg^{2+}, Ca^{2+}, Zn^{2+}, Cd^{2+}, Mn^{2+}, Co^{2+}, Cu^{2+}, and Ni^{2+}; 3 mM) and a 1:1 combination of Mg^{2+} and Ca^{2+} (1.5 mM Mg^{2+} + 1.5 mM Ca^{2+}). EDTA (3 mM) was applied to chelate divalent ions of Mg^{2+} and/or Ca^{2+}. Each column is the mean of three independent experiments, and error bars represent SE. Columns with different letters showed significant differences, with $P < 0.05$.

(22°C; Fig. 4B). In addition, we found that the transcript abundance of seven intrinsic Arabidopsis apyrase genes, *AtAPY1*, *AtAPY2*, *AtAPY3*, *AtAPY4*, *AtAPY5*, *AtAPY6*, and *AtAPY7*, was not altered by the overexpression of exogenous *PeAPY2* (Supplemental Fig. S6). Three series of cold treatments were carried out to determine the cold tolerance of *PeAPY2*-transgenic plants. Seedlings were subjected to increasing cold stress, with temperatures declining from 4°C (7 d) to −1°C (6 h) and then to −6°C (2 h; Chinnusamy et al., 2003; Yang et al., 2010). In this study, to avoid the rapid formation of ice and mechanical injury caused by ice crystallization (Scarth, 1944), cold-acclimated plants were used for freezing temperatures (Chinnusamy et al., 2003; Yang et al., 2010). At the tested temperatures, root length and electrolyte leakage were measured (Figs. 4 and 5). Plant recovery was measured after seedlings were returned to 22°C from cold incubation at either −1°C or −6°C. The temperature was gradually elevated to avoid rapid deplasmolysis and rupture of the protoplast caused by a rapid thawing (Scarth, 1944).

PeAPY2-OE2 and *PeAPY2-OE4* exhibited greater tolerance to low temperatures and showed greater recovery from cold stress, in terms of survival rate (Fig. 4C), root growth, electrolyte leakage, cell viability, and membrane integrity (Fig. 5). Specifically, at 4°C, the root lengths of wild-type seedlings, vector controls, and transgenic lines were suppressed by cold stress (4°C for 7 d), but wild-type and vector control seedlings showed the most pronounced reductions (Fig. 5B). At −1°C, fluorescein diacetate (FDA) and FM4-64 [*N*-(3-triethylammoniumpropyl)-4-(*p*-diethylaminophenyl-hexatrienyl) pyridinium dibromide] staining showed the effects of low temperature on cell viability and membrane integrity in the elongation zone of roots (Fig. 5A). Wild-type and transgenic plants grown in control conditions (22°C) showed clear FDA fluorescence within the cytoplasm, and FM4-64 fluorescence remained at the surface of root cells. These features indicated that cells were viable and retained membrane integrity. However, in cold-treated wild-type plants (−1°C for 12 h, then 4°C for 12 h; Fig. 5A), FDA fluorescence was undetectable in a number of root cells. We noted that FM4-64 rapidly (within 1 min) entered the cell and stained the entire endomembrane system, leading to a remarkable increase of FM4-64/FDA (Fig. 5A). This was due to impaired PM integrity. The vector control response to cold stress was similar to that observed in wild-type plants (data not shown). Compared with wild-type plants, *PeAPY2*-transgenic lines retained membrane integrity and cell viability during the period of cold stress; in transgenic cells, FDA fluorescence was visualized in root cells while FM4-64 fluorescence remained largely at the cell surface (Fig. 5A). Moreover, FM4-64/FDA in transgenic lines was significant lower than that in the wild type under the cold treatment (Fig. 5A). At −6°C, after exposure to

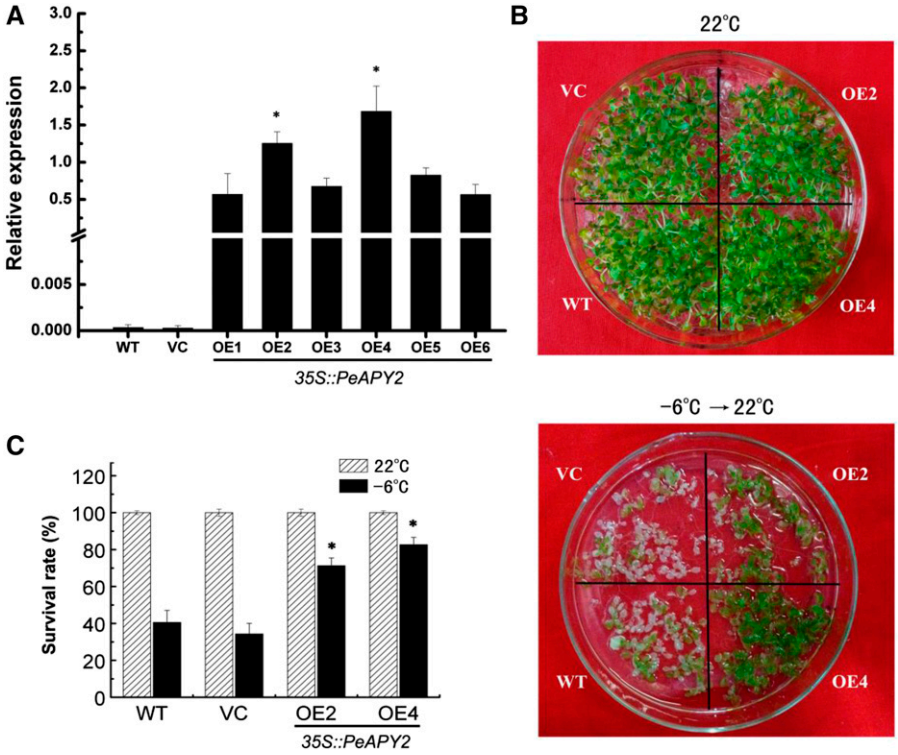

Figure 4. Cold tolerance of wild-type (WT), vector control (VC), and *PeAPY2*-transgenic (OE) Arabidopsis lines. A, qRT-PCR analysis results show the relative expression of *PeAPY2* compared with the expression of the Arabidopsis housekeeping gene, *ACTIN2*. Columns labeled with asterisks denote significant differences at $P < 0.05$ between transgenic lines. B and C, Freeze tolerance tests show responses of wild-type and transgenic plants. Seeds from wild-type, vector control, and transgenic lines (OE2 and OE4; T3 generation) were allowed to germinate on one-half-strength MS medium. Seven-day-old seedlings of all tested lines were acclimated at 4°C for 1 week and then transferred to a programmed freezing chamber. Petri dishes were maintained at −1°C for 6 h, and then the temperature was lowered to −6°C at a rate of 1°C h^{-1}. After 2 h of freezing treatment, the plates were removed to 4°C in the dark for 12 h and then transferred to 22°C under light for recovery. The survival rates of cold-stressed plants were measured after 10 d of recovery. Control plants were grown at 22°C in a long-day light period. Representative images (B) show plant performance before (top) and after (bottom) cold stress at −6°C. Survival rates (C) after recovery from freezing (−6°C) were compared with controls maintained at 22°C (100% survival). Each column is the mean of three independent experiments, and error bars represent SE. *, $P < 0.05$ for the wild type and vector controls versus transgenic lines after cold and recovery treatment.

increasing cold treatment (4°C for 7 d, then −1°C for 6 h, then −6°C for 2 h), plants were allowed 10 d of recovery (4°C for 12 h in dark, then 22°C for 10 d). The *PeAPY2*-transgenic lines showed a significantly higher survival rate (71%–83%) than wild-type and vector control plants (34%–41%; Fig. 4, B and C). This was partly due to the low electrolyte leakage from transgenic plants during the recovery period. Electrolyte leakage of wild-type seedlings and vector controls markedly increased by 3.4-fold after cold exposure, compared with seedlings grown in control conditions (Fig. 5C). However, the two transgenic lines (OE2 and OE4) showed less leakage than the vector control and wild-type plants during the recovery period (Fig. 5C).

PeAPY2 Overexpression Enhanced Vesicular Trafficking in Arabidopsis Roots

The low electrolyte leakage in cold-stressed transgenic lines suggested that disruptions in the PM were repaired to maintain membrane integrity. PM resealing requires the retrieval of wound sites from the PM (Idone et al., 2008) and exocytotic addition of internal membrane to the cell PM (Reddy et al., 2001; Schapire et al., 2009). Therefore, we investigated the effect of *PeAPY2* overexpression on vesicular trafficking in Arabidopsis. The fluorescent marker FM4-64 was used to track intracellular vesicular trafficking. FM4-64 can be efficiently inserted into the PM and taken up by endocytosis (Wang et al., 2005; Zonia and Munnik, 2008). We incubated the roots of Arabidopsis seedlings in FM4-64 (5 μM) for 10 min, then washed for 15 or 30 min. After 15 min of washing, the PM was stained with FM4-64 and intracellular endosomal bodies were labeled with internalized FM4-64 dye (Fig. 6A). The uptake of FM4-64 was more pronounced after 30 min of washing (Fig. 6B), indicating continuous endocytosis. Compared with wild-type cells, *PeAPY2-OE2* and *PeAPY2-OE4* cells exhibited more pronounced FM4-64 internalization, regardless of the wash duration (Fig. 6,

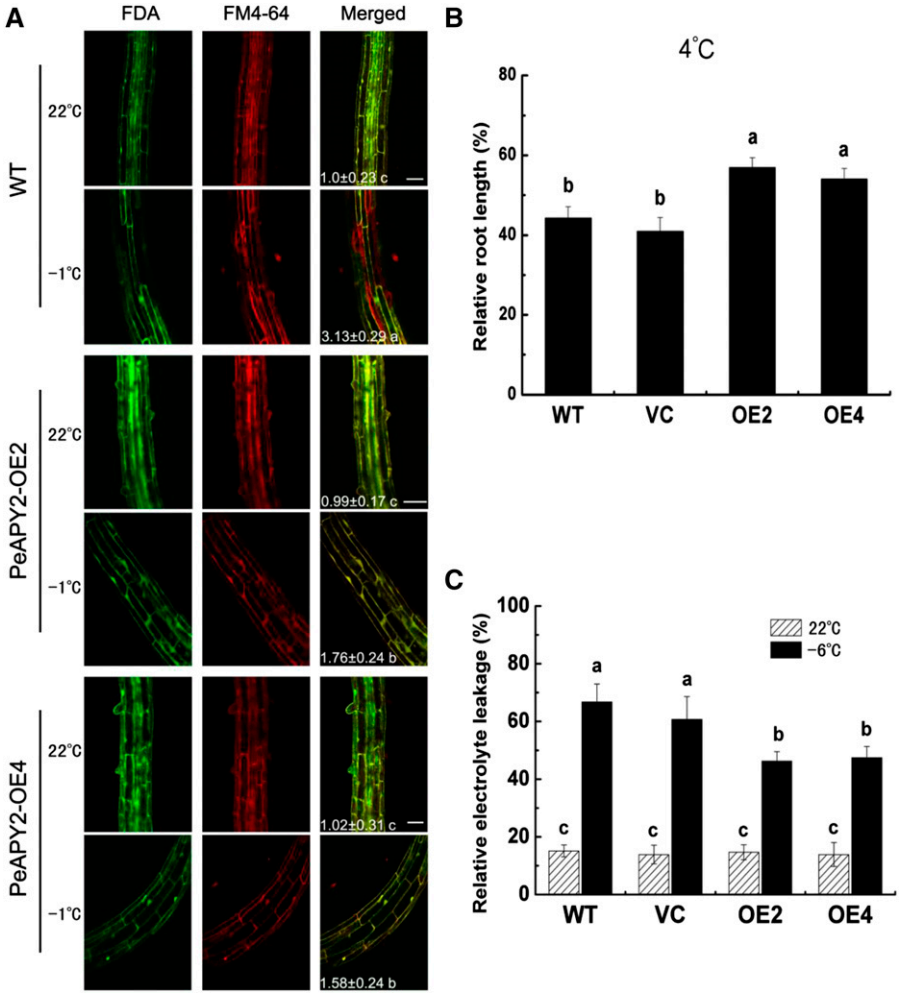

Figure 5. Effects of cold stress on root length, cell viability, and electrolyte leakage in wild-type (WT), vector control (VC), and *PeAPY2*-transgenic (OE) Arabidopsis lines. A, Cell viability. T3 seeds of wild-type, vector control, and *PeAPY2*-transgenic (OE2 and OE4) lines were germinated on one-half-strength MS medium. Seven-day-old seedlings of all tested lines were cold acclimated for 7 d and freezing treated at −1°C for 12 h. Thereafter, the seedlings were removed to 4°C for 12 h. Control plants were grown at 22°C in a long-day light period. Cell viability was assayed with fluorescein diacetate (FDA; green) and FM4-64 (red) double staining; representative images of the elongation zone of roots are shown. The ratio of FM4-64 to FDA fluorescence was calculated, and values were normalized to the wild-type control at 22°C. Values ± SD labeled with different letters showed significant differences at $P < 0.05$. Bars = 30 μm. B, Root length. Seven-day-old seedlings of wild-type, vector control, and *PeAPY2*-transgenic lines (T3 generation) were maintained at 4°C for 1 week. Root lengths of plants exposed to cold stress (4°C for 7 d) are expressed relative to non-cold-stressed controls (100%) of the same strains. C, Electrolyte leakage. Seven-day-old seedlings of all tested lines were acclimated at 4°C for 1 week and then subjected to an increasing freezing stress. Seedlings were exposed to −1°C for 6 h, and then the temperature was lowered to −6°C at a rate of 1°C h^{-1}. After 2 h of −6°C treatment, plants were removed to 4°C in the dark for 12 h and then transfer to 22°C under light for recovery. Electrolyte leakage of cold-stressed plants was measured after 3 d of recovery. Control plants were grown at 22°C in a long-day light period. In B and C, each column is the mean of three independent experiments, and error bars represent SE. Columns labeled with different letters showed significant differences at $P < 0.05$.

A and B). Therefore, the expression of *PeAPY2* conferred increased endocytosis in Arabidopsis root cells.

We used pharmacological treatments to confirm that the enhancement in vesicular trafficking was dependent on PeAPY2. Polyclonal antibodies against PeAPY2 were applied to inhibit PeAPY2 activity in transgenic plants, and NGXT191, a strong inhibitor of Arabidopsis apyrases, was used in wild-type plants. Roots were preincubated with NGXT191 (wild type) or anti-PeAPY2 antibodies (*PeAPY2*-transgenic lines) for 1.5 h. Then, FM4-64 was applied, and after 30 min of washing, fluorescent dye uptake in wild-type and transgenic plants was examined. The results showed that both NGXT191 and anti-PeAPY2 antibodies efficiently reduced FM4-64 uptake in root intracellular vesicles of wild-type and transgenic cells, respectively (Fig. 6C;

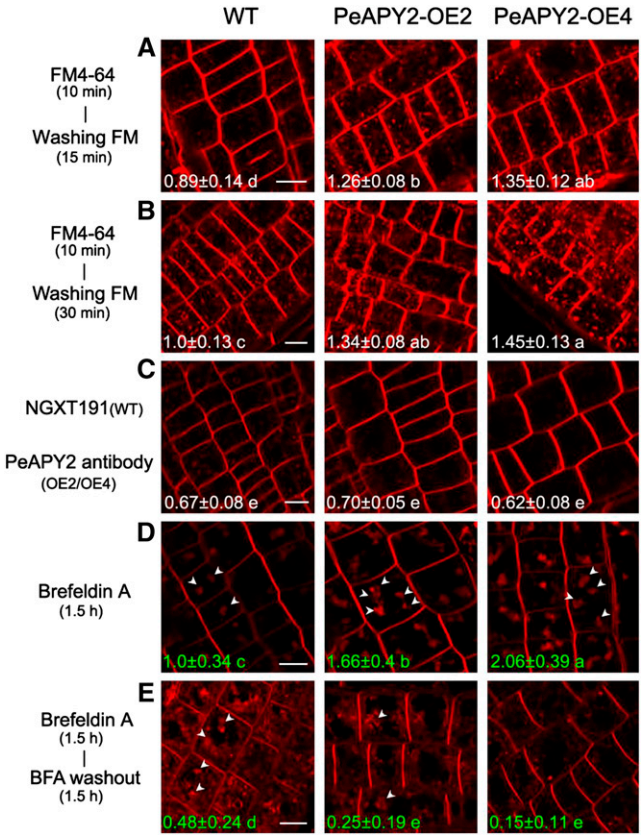

Figure 6. Effects of apyrase inhibitors and brefeldin A (BFA) on vesicular trafficking in root cells of wild-type (WT) and *PeAPY2*-transgenic plant lines. T3 seeds of wild-type and *PeAPY2*-transgenic lines (OE2 and OE4) were germinated on one-half-strength MS medium, and 7-d-old seedlings of all tested lines were used for FM4-64 staining (red). A and B, Endocytosis. Seedlings were stained with FM4-64 for 10 min and then washed for 15 min (A) or 30 min (B). Endocytic vesicles are stained red. C, Apyrase inhibitor treatment. Prior to FM4-64 staining, wild-type roots were treated with NGXT191 (3 μg mL^{-1}), and *PeAPY2*-transgenic lines were treated with polyclonal antibodies against PeAPY2 at a dilution of 1:500, for 1.5 h. The uptake of FM4-64 was calculated as the ratio of intracellular fluorescence to whole-cell fluorescence, and values were standardized to the wild-type control with 30 min of washing of FM4-64. In A to C, values ± SD labeled with different letters showed significant differences at $P < 0.05$. D and E, Exocytosis. After FM4-64 staining, wild-type and transgenic plant roots were incubated with BFA (50 μM for 1.5 h). Images show FM4-64 uptake before (D) and after (E) washing out BFA for 1.5 h. Arrowheads indicate BFA bodies. BFA bodies were quantified as the ratio of intracellular surface to the whole cell, and values were standardized to the wild-type control before BFA washing. Values ± SD labeled with different letters showed significant differences at $P < 0.05$. Bars = 10 μm.

Supplemental Fig. S7). FM4-64 internalization was not affected when the same concentrations of the solvent dimethyl sulfoxide and preimmune serum were applied to roots (data not shown). These findings indicated that vesicular trafficking suppression in wild-type and transgene plants was due to apyrase inhibition by NGXT191 and PeAPY2 antibodies, respectively. In addition, we noticed that, in *PeAPY2*-transgenic lines, NGXT191 did not significantly suppress FM4-64 uptake in root cells at the tested concentrations, 1.5, 3, and 6 μg mL^{-1} (Supplemental Fig. S7). This finding was consistent with the result by in vitro measurement (Fig. 3B).

Next, we tested whether PeAPY2 could stimulate exocytosis. We monitored FM4-64 uptake and trafficking in the presence of BFA, which inhibits intracellular vesicular trafficking and peptide secretion (Lam et al., 2009; Feraru et al., 2012). We stained Arabidopsis roots with FM4-64 (10 min) prior to BFA treatment (50 μM for 1.5 h). We clearly detected aggregations of vesicles, or BFA bodies, within cells (Fig. 6D). BFA bodies formed and expanded with continuous endocytosis, because exocytosis was blocked by BFA. Compared with wild-type plants, transgenic lines exhibited larger and more abundant BFA bodies (Fig. 6D), which indicated vigorous endocytosis, because BFA had no significant inhibition of FM4-64 internalization (Supplemental Fig. S8). Interestingly, a low dose of BFA (10 μM) stimulated FM4-64 uptake in the wild type, which is similar to the findings in tobacco (*Nicotiana tabacum*) BY-2 suspension cells (Emans et al., 2002). However, 1-naphthaleneacetic acid (NAA), a typical inhibitor of endocytosis (Paciorek et al., 2005), suppressed FM4-64 internalization in Arabidopsis roots, but with a more pronounced effect in the wild type compared with transgenic plants (Supplemental Fig. S8). We then tested the restoration of exocytosis after BFA washout (1.5 h of washing). Washing significantly reduced the number and size (indicated by surface area) of BFA bodies in *PeAPY2-OE2* and *PeAPY2-OE4* lines (Fig. 6E). However, in wild-type roots, BFA bodies remained detectable, although smaller (Fig. 6E). These observations suggested that PeAPY2 overexpression in Arabidopsis enhanced both endocytosis and exocytosis.

PeAPY2 Enhanced Vesicular Trafficking in Cold-Stressed Arabidopsis Roots

Under control growth conditions (22°C), FM4-64 uptake was more evident in root cells of *PeAPY2*-transgenic lines compared with roots of wild-type seedlings (Fig. 7A). Cold stress (4°C for 24 h) significantly reduced vesicular trafficking (indicated by internalized FM4-64 dye) in root cells, but the effect was less pronounced in transgenic lines than in the wild type (Fig. 7B). This result was consistent with the finding that transgenic plants maintained PM integrity after recovery from freezing stress (Fig. 5). We performed pharmacological experiments to test whether *PeAPY2*-transgenic plants could maintain vesicular trafficking during the recovery process. Seedlings of wild-type and transgenic lines were cold acclimated (4°C for 7 d) and then exposed to −1°C (6 h); this treatment was followed by a recovery procedure (4°C for 12 h in the dark, then 22°C for 1 d); next, trafficking was assessed in an FM4-64 assay. We applied BFA for 90 min to inhibit exocytosis. In root cells of wild-type plants, a single, huge BFA body was observed (Fig. 7C). This

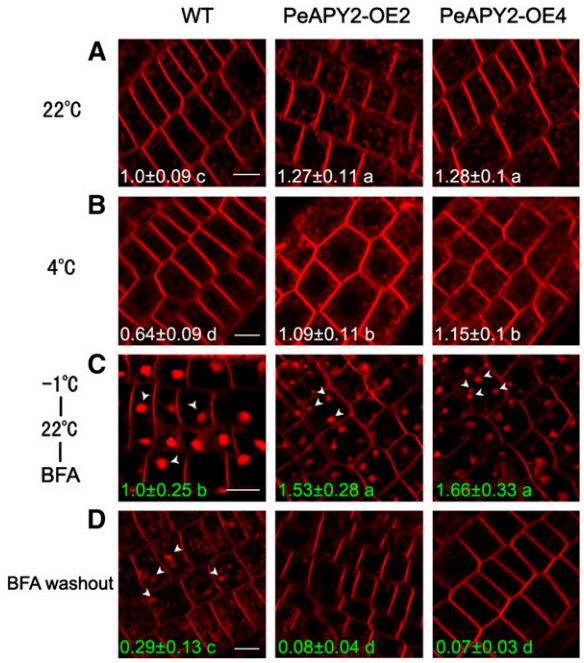

Figure 7. Effects of low temperatures on vesicular trafficking in root cells of wild-type (WT) and *PeAPY2*-transgenic lines. A and B, T3 seeds of wild-type and *PeAPY2*-transgenic lines (OE2 and OE4) were germinated on one-half-strength MS medium. Seven-day-old plants were cultured under control growth conditions at 22°C (A) or exposed to 4°C for 24 h (B). Control and cold-stressed roots were stained with FM4-64 for 10 min, followed by a 30-min washing. The uptake of FM4-64 was calculated as the ratio of intracellular fluorescence to whole-cell fluorescence, and values were standardized to the wild-type control. Values ± SD labeled with different letters showed significant differences at $P < 0.05$. C and D, Seven-day-old seedlings were cold acclimated (4°C for 7 d) and then exposed to −1°C for 6 h. Next, the seedlings were moved to 4°C for 12 h in the dark and then allowed to recover at 22°C for 1 d. After FM4-64 staining, roots of wild-type and transgenic lines were incubated with BFA (50 μM for 1.5 h). Images show FM4-64 uptake before (C) and after (D) washing out BFA for 1.5 h. Arrowheads indicate BFA bodies. BFA bodies were quantified as the ratio of intracellular surface to the whole cell, and values were standardized to the wild-type control before BFA washing. Values ± SD labeled with different letters showed significant differences at $P < 0.05$. Bars = 10 μm.

resulted from endocytosis in the absence of exocytosis. In root cells of transgenic plants, several BFA bodies were observed: their total surface area was larger than in the wild type, although they were relatively smaller in size (Fig. 7C). When the BFA was washed out for 1.5 h, no BFA bodies were observed in *PeAPY2-OE2* and *PeAPY2-OE4* lines (Fig. 7D). The disappearance of BFA bodies indicated that the accumulated endosomal compartments were delivered to the PM via exocytosis. In contrast to transgenic plants, wild-type plants retained BFA bodies after BFA was washed out (Fig. 7D). Collectively, these results indicated that transgenic plants retained a higher capacity than wild-type plants for regulating vesicular trafficking, and this capacity favored membrane repair during cold stress and recovery.

PeAPY2 Controlled eATP Concentrations under Cold Stress and Recovery

To determine whether PeAPY2 could control eATP concentrations in cold-stressed roots, we measured eATP concentrations with a luciferin-luciferase assay (Sun et al., 2012b). For the first 2 d of cold exposure, [eATP] steadily increased in all tested plants (Fig. 8A). However, on day 4, wild-type roots exhibited significantly higher [eATP] than the *PeAPY2*-transgenic lines (Fig. 8A). After plants were removed from cold conditions for 12 h, wild-type roots sustained 37% higher [eATP] than transgenic roots (Fig. 8A). These results suggested that Arabidopsis plants that overexpressed *PeAPY2* retained a greater capacity to control the eATP than wild-type plants, due to the ATP hydrolysis activity of PeAPY2 (Fig. 3).

High eATP Levels Suppressed Cell Viability in Arabidopsis Roots

A previous study showed that high levels of eATP could reduce viability and increase programmed cell death in *P. euphratica* cells (Sun et al., 2012a). To determine whether cold-elicited increases in eATP could induce cell death, we examined the effects of high eATP on root cell viability under normal (22°C) and low-temperature (−6°C) conditions. At 22°C, under control conditions, viable cells displayed green fluorescence due to stronger FDA staining (green) than propidium iodide (PI) fluorescence (red), and the abundance of viable cells was similar in wild-type and transgenic plants (Fig. 8B). After exposure to high eATP (800 μM) for 12 h, wild-type roots showed weak FDA fluorescence along the roots, particularly in the transition and elongation zones (Fig. 8B; Supplemental Fig. S9A). With PI staining, wild-type cells displayed orange fluorescence at the root cap and PI-stained nuclei were observed in the elongation and mature regions (Fig. 8B). Compared with the wild type, ATP induction of root cell death was less pronounced in *PeAPY2*-transgenic lines than in wild-type plants, because the ATP-treated transgenic plants displayed higher FDA fluorescence and less PI staining along the root axis (Fig. 8B; Supplemental Fig. S9A). However, nonhydrolyzable ATP, ATPγS (800 μM), was stronger than hydrolyzable ATP for triggering cell death in both transgenic and wild-type plants (Supplemental Fig. S10). At −6°C, under cold stress conditions, there were also marked differences in ATP induction of root cell death between wild-type and *PeAPY2*-transgenic lines. *PeAPY2*-transgenic plants retained typically higher FDA fluorescence than the wild type under cold stress (Fig. 9; Supplemental Fig. S9B). ATP (50 or 600 μM) increased PI fluorescence (red) in cold-stressed roots, but the effect was more pronounced in the wild type than in the transgenic lines (Fig. 9). In our study, the products of apyrase (i.e. ADP, AMP, and PO_4^{3-}) had no significant effect on cell death at the tested concentrations (0, 50, 600, or 800 μM), irrespective of temperature treatments at 22°C (Supplemental Fig. S9A) or −6°C (Supplemental

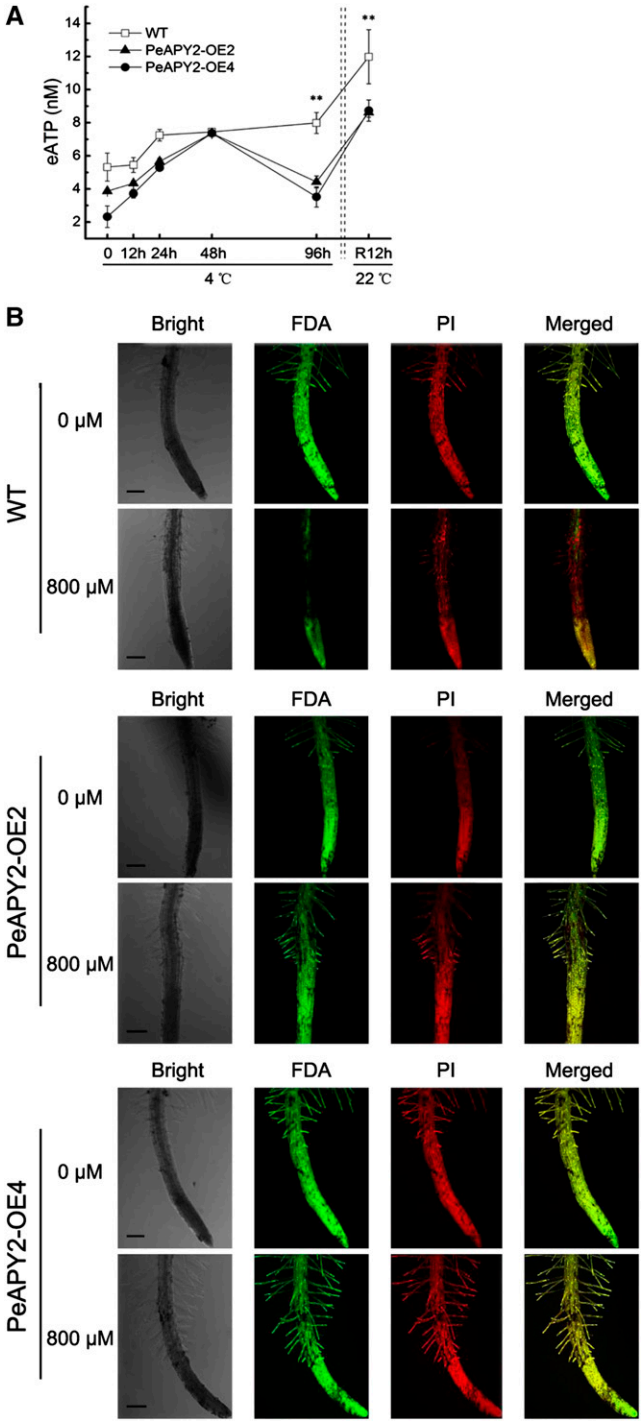

Figure 8. Effects of cold stress on eATP concentrations and eATP inhibition of cell viability in wild-type (WT) and *PeAPY2*-transgenic lines. T3 seeds of wild-type and *PeAPY2*-transgenic lines (OE2 and OE4) were germinated on one-half-strength MS medium. A, Seven-day-old seedlings of all tested lines were subjected to 4°C for 7 d (cold stress), followed by −1°C for 12 h and 4°C for 12 h, and were finally returned to 22°C for 12 h of recovery (R12h). [eATP] was measured in extracellular root medium. Each point is the mean of three independent experiments, and error bars represent SE. **, $P < 0.01$, wild-type versus *PeAPY2*-transgenic lines. B, eATP inhibition of cell viability. Seven-day-old seedlings of wild-type and *PeAPY2*-transgenic lines (OE2 and OE4) were treated with 0 or 800 μM ATP for 12 h. Equal molar values of $CaCl_2$ were applied for the ATP treatment, and pH was adjusted to 5.7 to 5.8 when ATP was added into the nutrient solution. Root cell viability was assayed with FDA (green) and PI (red) staining. The merged images show the double staining. Three independent experiments were performed, and representative images are shown. Bars = 250 μm.

Fig. S9B). This agrees with the result of Sun et al. (2012a), who found that the ATP metabolic products did not induce cell death in *P. euphratica* cells.

eATP Mediates Dose-Dependent Vesicular Trafficking in Arabidopsis Roots

eATP has dual functions in plant cell signaling. These functions are largely dependent on the ATP concentration in the ECM (Clark et al., 2010a, 2011; Sun et al., 2012a). Our data showed that high eATP could reduce cell viability in Arabidopsis roots (Fig. 8B; Supplemental Fig. S9). This effect was also found in *P. euphratica* cells (Sun et al., 2012a). Next, we investigated whether the eATP effect on viability was correlated to vesicular trafficking in Arabidopsis roots. Our FM4-64 internalization experiments showed that low doses of eATP (20 or 50 μM) enhanced vesicular trafficking in wild-type Arabidopsis (Fig. 10; Supplemental Fig. S11). The ATP induction of trafficking in transgenic lines was not as pronounced as that in wild-type cells (Fig. 10; Supplemental Fig. S11), because transgenic plants exhibited high baseline trafficking in the absence of low ATP doses (Figs. 6, 7, and 10). When we exposed plants to higher doses of eATP (500 or 1,000 μM), we observed significant reductions in FM4-64 internalization in both wild-type and *PeAPY2*-transgenic lines (Fig. 10; Supplemental Fig. S11); however, wild-type seedlings showed more pronounced reductions than transgenic seedlings (Fig. 10; Supplemental Fig. S11). The reduction in vesicular trafficking was more pronounced at 1,000 μM than at 500 μM eATP (Fig. 10). Moreover, the nonhydrolyzable ATP analog, ATPγS (500 μM), diminished FM4-64 internalization to a similar extent in both wild-type and *PeAPY2*-transgenic lines (Fig. 10). This indicated that eATP hydrolysis by abundant PeAPY2 alleviated the eATP-induced inhibition of vesicular trafficking. In this study, the products of apyrase action, ADP, AMP, and PO_4^{3-}, had no significant effect on vesicle trafficking at the tested concentrations, 20, 50, 500, or 1,000 μM (Supplemental Fig. S11), suggesting that ATP-diminished trafficking is not attributable to ATP metabolites.

DISCUSSION

PeAPY2 Localization and Apyrase Activity

Our phylogenetic analysis indicated that PeAPY2 was homologous to apyrases in various plant species (Supplemental Fig. S3). Subcellular localization of

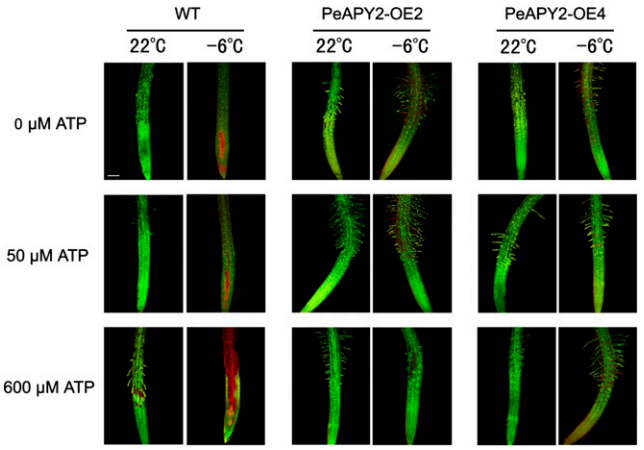

Figure 9. Effects of ATP on viability in root cells of wild-type (WT) and *PeAPY2*-transgenic lines under cold stress. T3 seeds of wild-type and *PeAPY2*-transgenic lines (OE2 and OE4) were germinated on one-half-strength MS medium. Roots of wild-type and transgenic seedlings (7 d old) were exposed to 0, 50, or 600 μM ATP for 24 h. Equal molar values of $CaCl_2$ were applied for the ATP treatment, and pH was adjusted to 5.7 to 5.8 when ATP was added into the nutrient solution. These seedlings of wild-type and transgenic lines were cold acclimated at 4°C for 1 d and subjected to low-temperature treatment: −1°C for 16 h, then the temperature was lowered to −6°C for 2 h and finally recovered at 4°C for 12 h. Control plants were grown at 22°C in a long-day light period. Then, roots were stained with FDA (green) and PI (red) to examine root cell viability with a confocal microscope. Three independent experiments were performed, and representative images are shown. Bar = 10 μm.

PeAPY2 in onion and Arabidopsis showed that PeAPY2 was mainly localized to the PM (Fig. 2). The colocalization assay in Arabidopsis protoplasts showed that PeAPY2 also resided in the ER and Golgi apparatus (Fig. 2). Localization analysis of apyrase reveals species differences in subcellular localization. The potato-specific apyrase is apoplastically localized and plays a crucial role in regulating growth and development (Riewe et al., 2008). Fractionation of cellular membranes and subsequent western analysis of the fractions revealed that soybean (*Glycine max*) GS52 localized in the PM (Day et al., 2000). Recent studies revealed that two apyrase homologs in Arabidopsis, AtAPY1 and AtAPY2, were localized to the Golgi apparatus, and both were involved in protein glycosylation and cell wall polysaccharide synthesis (Chiu et al., 2012; Schiller et al., 2012; Lim et al., 2014; Massalski et al., 2015). It is also possible that Arabidopsis apyrases function as ectoapyrases on the PM, as the growth of pollen tubes was suppressed by externally applied polyclonal antibodies against AtAPY1 and AtAPY2 (Wu et al., 2007). PeAYP2 was predicted to be a secretory protein with PSORT (http://psort.hgc.jp/form.html) and the secretomeP server (http://www.cbs.dtu.dk/services/SecretomeP/). The localization of PeAPY2 to multiple sites has been observed for other secretory proteins (Schapire et al., 2008; Han et al., 2013). We propose that PeAPY2 is likely produced in the ER and transported through the Golgi to the PM. In accordance, immunolabeling studies showed that multivesicular bodies were also positively immunolabeled by gold particles, which most likely reflects the transport of AtAPY1 (Schiller et al., 2012). The species-specific localizations of the apyrases are presumably due to the sequence difference, especially in the uncleaved signal sequence at the N terminus (Supplemental Fig. S2), which serves as a transmembrane anchor (Schiller et al., 2012).

An amino acid sequence analysis showed that PeAPY2 harbored five intact apyrase-conserved regions (ACRs; Supplemental Fig. S2), which are highly conserved in both animals and plants (Knowles, 2011;

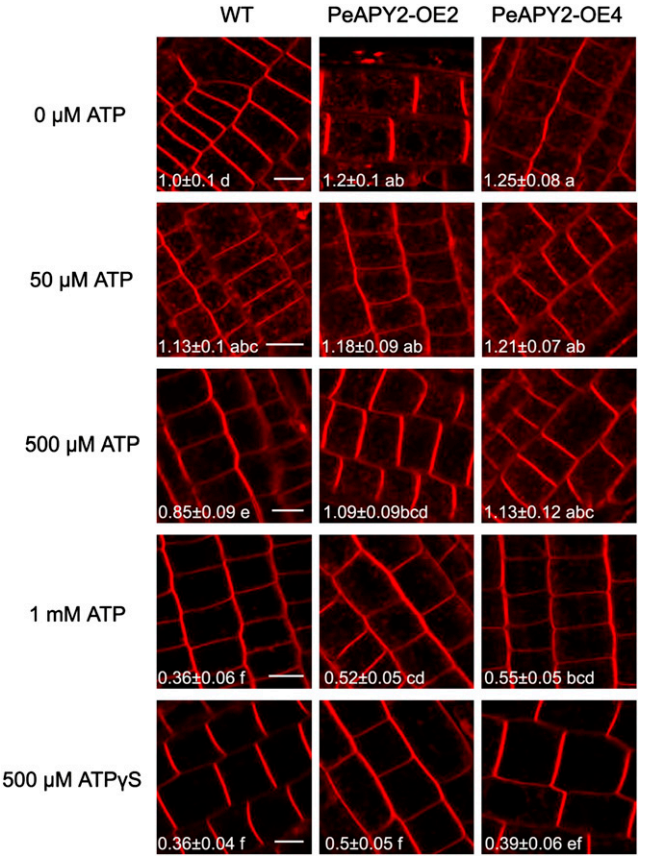

Figure 10. Effects of hydrolyzable ATP and nonhydrolyzable ATPγS on vesicular trafficking in root cells of wild-type (WT) and *PeAPY2*-transgenic lines. T3 seeds of wild-type and *PeAPY2*-transgenic lines (OE2 and OE4) were germinated on one-half-strength MS medium. Seven-day-old seedlings were exposed to different concentrations of eATP (0, 50, 500, and 1,000 μM) or extracellular ATPγS (500 μM) for 1.5 h. Equal molar values of $CaCl_2$ were applied for the ATP treatment, and pH was adjusted to 5.7 to 5.8 when ATP was added into the nutrient solution. Then, roots were stained with FM4-64 for 10 min and washed for 30 min. Three independent experiments were performed, and representative images are shown. The uptake of FM4-64 was calculated as the ratio of intracellular fluorescence to whole-cell fluorescence, and values were standardized to the wild-type control treated without ATP or ATPγS. Values ± SD labeled with different letters showed significant differences at $P < 0.05$. Bars = 10 μm.

Schiller et al., 2012; Okuhata et al., 2013). The highly conserved nucleotide-binding domains, ACR1 and ACR4, are essential for enzymatic activity (Tanaka et al., 2011). The PeAPY2 enzyme exhibited broad substrate specificity (Fig. 3), similar to the soybean ectoapyrase, GS52 (Tanaka et al., 2011), the pea (*Pisum sativum*) apyrase, PsAPY1 (Cannon et al., 2003), the cowpea (*Vigna sinensis*) apyrase, Nucleotide Phosphohydrolases1 (VsNTPase1; Takahashi et al., 2006), and the *Dolichos biflorus* ectoapyrase (Etzler et al., 1999). The ATP-hydrolyzing activity of PeAPY2 (V_{max} = 70.8 ± 9.4 μmol h^{-1} mg^{-1}; Supplemental Fig. S4) was higher than that of GS52 (V_{max} = 38.2 ± 1.9 μmol h^{-1} mg^{-1}; Tanaka et al., 2011). PeAPY2 also showed higher affinity for ATP (K_m = 390 ± 12 μM; Supplemental Fig. S4) as compared with GS52 (K_m = 424 ± 24 μM; Tanaka et al., 2011). PeAPY2 displayed higher enzymatic activity on purine nucleotides (ATP and GTP) than on pyrimidine nucleotides (CTP and UTP) or diphosphate nucleotides (e.g. ADP and UTP; Fig. 3). This result was different from observations with GS52, which showed higher enzymatic activity on pyrimidine nucleotides and diphosphate nucleotides than on ATP (Tanaka et al., 2011). Recently, Massalski et al. (2015) showed that GDP, IDP, and UDP, instead of ATP, were hydrolyzed by AtAPY1. Moreover, our pharmacological experiments showed that the PeAPY2 catalytic domain was likely located on the extracellular surface. We found that *PeAPY2* overexpression in Arabidopsis enhanced vesicular trafficking in root cells (Fig. 6), and this enhancement was efficiently inhibited with the anti-PeAPY2 antibody (Fig. 6). Because the PM is not permeable to antibodies, we assumed that the polyclonal antibodies must have bound to extracellular epitopes of PeAPY2 to block its nucleotide-hydrolyzing activity (Wu et al., 2007). However, at present, we cannot exclude a possible role for the apyrase in eATP control in the Golgi, since PeAPY2 also has a Golgi localization (Fig. 2; Chiu et al., 2012; Schiller et al., 2012; Massalski et al., 2015). It is suggested that apyrase could indirectly control [eATP] through the regulation of the luminal concentration of ATP ([ATP]) in secretory vesicles derived from the Golgi (Lim et al., 2014). Furthermore, PeAPY2 showed an evident activity toward GTP (Fig. 3), indicating that the apyrase is likely involved in regulating protein glycosylation (Abeijon et al., 1993; Gao et al., 1999). Yeast apyrases, which control the turnover of GTP, are shown to regulate protein glycosylation and cell wall integrity (Abeijon et al., 1993; Gao et al., 1999). In *PeAPY2*-transgenic Arabidopsis, the high density of endosome (Figs. 6, 7, and 10) reflects the enhanced transport of secretory vesicles. Golgi-derived vesicles have been implicated in the process of membrane repair (Reddy et al., 2001). Thus, it can be inferred that in *PeAPY2*-transgenic Arabidopsis, the enhanced transport of Golgi-derived secretory vesicles provides PM materials (e.g. glycoprotein and glycolipid) for membrane repair.

We showed that PeAPY2 apyrase activity increased with divalent ion cofactors, particularly Mg^{2+} (Fig. 3). Similarly, Mg^{2+} was the preferred cofactor for ectonucleotidase in human hepatocellular carcinoma (HepG2) cells (Fujii et al., 2012), but GS52 apyrase showed a preference for Ca^{2+} as a cofactor (Tanaka et al., 2011). PeAPY2 activity was not sensitive to inhibitors for various types of ATPases, including pyrophosphatase, F-, V-, and P-type ATPases, and acid phosphatase (Fig. 3). This feature was common to apyrases in other plant species (Okuhata et al., 2011; Tanaka et al., 2011). We showed that PeAPY2 activity was not suppressed by NGXT191 (Fig. 3), a strong inhibitor for apyrases in Arabidopsis. Moreover, NGXT191 could not suppress *P. euphratica* apyrase in vivo (*PeAPY2*-transgenic lines; Supplemental Fig. S7). Similarly, NGXT191 had no inhibitory effect on GS52 apyrase activity (Tanaka et al., 2011). These findings implied that apyrases originated from cold-resistant woody plants and that rhizobium-legume symbiosis differs from apyrases that dominate in mediating growth regulation in Arabidopsis.

PeAPY2 Enhanced Cold Tolerance and Recovery from Cold Stress

The cold induction of *PeAPY2* indicated that PeAPY2 could contribute to cold tolerance in *P. euphratica* (Fig. 1). Accordingly, *PeAPY2* overexpression in Arabidopsis enhanced plant cold tolerance in terms of root growth and survival rate (Figs. 4 and 5). In wild-type plants, cold stress reduced root growth and cell viability, presumably by disrupting membrane integrity (Figs. 4 and 5). Compared with wild-type plants, *PeAPY2*-transgenic plants exhibited greater cell viability, membrane integrity, and root length during cold stress (Figs. 4 and 5). Moreover, cold-treated transgenic plants exhibited less electrolyte leakage than wild-type plants during the recovery period (Figs. 4 and 5). These findings indicated that *PeAPY2*-transgenic plants could repair injured membranes caused by low temperatures.

PeAPY2 Modulated Vesicular Trafficking and eATP Levels under Cold Stress and Recovery

PM resealing requires the retrieval of wound sites from the PM (Idone et al., 2008) and the delivery of intracellular membranes by exocytosis (Togo et al., 1999; McNeil et al., 2003). Interestingly, *PeAPY2*-transgenic plants typically displayed vigorous endocytosis and exocytosis compared with wild-type plants (Fig. 6). FM4-64, an endocytic trafficking tracer (Bolte et al., 2004), showed that *PeAPY2*-transgenic plants also harbored a higher density of endosomes in root cells under cold stress conditions compared with wild-type plants (Fig. 7). Those results suggested that PeAPY2 enhanced endocytosis, which contributes to membrane repair by retrieving the wound site from the PM (Idone et al., 2008). Moreover, when exocytosis was inhibited with BFA, transgenic lines showed enhanced accumulation of BFA bodies, due to endocytosis (Fig. 6; Lam et al., 2009; Feraru et al., 2012). When BFA was removed, the

number of BFA bodies was significantly reduced in transgenic plants (Fig. 6). This indicated that *PeAPY2*-transgenic plants secreted endosomal vesicles to the PM. Cold exposure inhibited endocytosis in *PeAPY2*-transgenic plants less than in wild-type plants (Fig. 7). During recovery, root cell exocytosis was less sensitive to BFA in transgenic plants than in wild-type plants (Fig. 7). Moreover, exocytosis was rapidly restored in transgenic roots when BFA was removed from the root medium (Fig. 7). The secretory vesicles carrying glycoprotein, glycolipid, might transport to the PM and facilitate cell membrane resealing (Reddy et al., 2001). However, the anti-PeAPY2 antibodies markedly inhibited both endocytosis and exocytosis in transgenic plants (Fig. 6). Similarly, in *P. euphratica* cells, vesicular trafficking was also suppressed by the anti-PeAPY2 antibodies (data not shown). These findings indicated that PeAPY2 enhanced vesicular trafficking in *P. euphratica* and transgenic Arabidopsis.

Moreover, our data showed that PeAPY2 may reduce the eATP inhibition of trafficking by hydrolyzing ATP in the extracellular medium. High eATP (500–1,000 μM) or the nonhydrolyzable ATP (ATPγS; 500 μM) inhibited vesicular trafficking (Fig. 10), but low ATP (50 μM) accelerated trafficking (Fig. 10). The dual function of eATP has also been shown in stomatal movement (Clark et al., 2011), hypocotyl elongation (Roux et al., 2006), cotton fiber elongation (Clark et al., 2010a), root hair growth (Clark et al., 2010b), and Ca^{2+} flux (Demidchik et al., 2011). In those studies, high ATP doses caused stomatal closure, reduced the elongation of hypocotyl, cotton fiber, and root hair, and induced substantial Ca^{2+} loss (Demidchik et al., 2011). Similarly, in this study, we found that high eATP suppressed vesicular trafficking and reduced cell viability in Arabidopsis (Figs. 8 and 10; Supplemental Figs. S9 and S11). Cold treatment reduced membrane integrity (Fig. 5), which caused a significant rise in eATP levels around the roots (Fig. 8). Thus, in cold-stressed wild-type plants, it can be inferred that high eATP restricted vesicular trafficking and membrane repair in root cells (Fig. 7), which substantially reduced cell viability (Fig. 5). In accordance, the application of ATP (50 and 600 μM) significantly suppressed root cell viability under cold stress, although the effects were more pronounced in the wild type than in the transgenic lines (Fig. 9; Supplemental Fig. S9). At present, we cannot exclude the possibility that eATP may have induced programmed cell death, because excess eATP was found to initiate programmed cell death in plants (Sun et al., 2012a). Our data showed that *PeAPY2*-transgenic lines could hydrolyze eATP, because (1) eATP in transgenic root medium was lower than that in wild-type root medium under cold stress and recovery (Fig. 8) and (2) vesicular trafficking and cell viability were less inhibited in transgenic roots compared with wild-type roots when the same eATP concentration (50–1,000 μM) was applied under normal and low-temperature conditions (Figs. 9 and 10; Supplemental Figs. S9 and S11); but, vesicular trafficking and viability were similar in the two groups when nonhydrolyzable ATP (ATPγS; 500 or 800 μM) was applied (Fig. 10; Supplemental Fig. S10). That result indicated that ATP hydrolysis was required for transgenic plants to alleviate the effects of high eATP on vesicular trafficking and cell viability. Taken together, our results demonstrated that the overexpression of *PeAPY2* provided a means to efficiently hydrolyze eATP in root medium and avoid excessive ATP accumulation. This may benefit transgenic plants by reducing the eATP inhibition of vesicular trafficking and membrane repair under cold stress and recovery conditions.

In this study, eATP levels were in the nanomolar range in cold-stressed *P. euphratica* cells and Arabidopsis roots, as eATP levels were obtained by measuring [ATP] in the medium surrounding the plant materials (Kim et al., 2009; Weerasinghe et al., 2009). The actual [ATP] at the cell surface might be higher than the value in the sampled bulk medium (Weerasinghe et al., 2009). Song et al. (2006) measured ATP as high as 40 μM in wound sites of Arabidopsis rosette leaves. With a noninvasive ATP microbiosensor, Vanegas et al. (2015) detected an increase in the [eATP] to 3.4 μM after corn (*Zea mays*) roots were wounded. Using a cellulose-binding domain-luciferase reporter, eATP hotspots have been found in elongating root cells (Kim et al., 2006).

Low temperature suppressed vesicular trafficking in Arabidopsis roots (Fig. 7). It has been shown that intracellular trafficking of auxin efflux carriers was inhibited after the initiation of cold treatment (Shibasaki et al., 2009). The initial responses of plants to cold stress, such as root growth, gravity response, and auxin transport, occurred within hours (Shibasaki et al., 2009). In *P. euphratica*, the up-regulation of apyrase took 3 d to reach significant levels, which suggests that apyrase and eATP were involved in the cold response only after significant membrane leakage had occurred (Fig. 1).

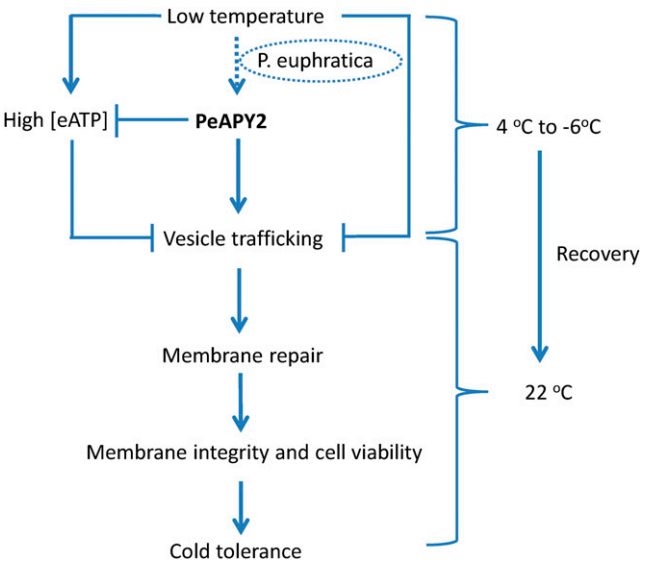

Figure 11. Schematic model showing the role of *P. euphratica* apyrase, PeAPY2, in cold tolerance and recovery from cold stress.

Therefore, the pattern of plant adaptation to low-temperature conditions differs from the initial response upon cold exposure. Based on our results, we hypothesized that PeAPY2 confers enhanced cold tolerance in *P. euphratica* by modulating vesicular trafficking and eATP levels during long-term cold stress. High eATP was found to inhibit vesicular trafficking (data not shown) and viability in *P. euphratica* cells (Sun et al., 2012a). Under long-term stress, the activated PeAPY2 enables *P. euphratica* to directly hydrolyze eATP in the ECM and/or control the [ATP] in Golgi-derived secretory vesicles (Lim et al., 2014), thus preventing the accumulation of eATP to levels that can inhibit vesicular trafficking and membrane repair and induce cell death. This confers the ability of *P. euphratica* cells to survive low temperatures and prolonged periods of cold stress. The critical control of eATP was shown previously in salt-stressed *P. euphratica*. In that study, NaCl shock elicited a significant rise in eATP in the ECM surrounding *P. euphratica* cells, but eATP levels returned to basal levels after 20 min of salt treatment (Sun et al., 2012b). This was presumably the result of ATP hydrolysis by apyrase, an extracellular nucleotide phosphohydrolase.

Furthermore, based on our findings, we propose a signaling pathway in which PeAPY2 mediates cold tolerance in transgenic Arabidopsis. As shown in Figure 11, cold treatment inhibits vesicular trafficking and increases electrolyte leakage in the PM, which results in ATP release to the ECM. The excess eATP inhibits vesicular trafficking and membrane repair, which leads to membrane disruption and decreased cell viability. When Arabidopsis plants overexpress PeAPY2, they show enhanced vesicular trafficking and highly active ATP hydrolysis, which then reduces the excess accumulation of cold-elicited eATP in the ECM. Thus, PeAPY2 protects membrane integrity, which benefits transgenic plant growth and survival during cold stress and recovery. In *P. euphratica* cells, *PeAPY2* was up-regulated under low-temperature conditions (Fig. 11). The activated PeAPY2 enhanced vesicular trafficking and modulated eATP levels to reduce the ATP inhibition of vesicular trafficking and membrane repair (Fig. 11).

MATERIALS AND METHODS

Plant Material Culture and Cold Treatment

Callus cells were induced from *Populus euphratica* shoots and subcultured as described previously (Sun et al., 2012b) with some modifications. Briefly, the calluses were grown on MS solid medium (2.5% [w/v] Suc, pH 6) that contained 0.5 mg L^{-1} 6-benzyladenine and 0.5 mg L^{-1} NAA. Cultures were raised in the dark at 25°C and subcultured every 15 d. After 10 d of transformation onto new MS medium, the calluses were used for cold treatments and RNA isolation.

P. euphratica cells were subjected to 4°C for cold treatment (7 d), and control cells were cultured at 25°C. Control and cold-stressed calluses were sampled to measure relative electrolyte leakage (Wang et al., 2007, 2008), malondialdehyde content (Wang et al., 2007, 2008), [eATP] (Sun et al., 2012b), and the expression of *PeAPY1* and *PeAPY2* (see below).

PeAPY2 Cloning

Total RNA was isolated from callus cells of *P. euphratica* with TRIzol reagent (Invitrogen). First-strand complementary DNA (cDNA) was synthesized with the SuperScript III first-strand synthesis system kit (Invitrogen) and oligo(dT) primers, according to the manufacturer's instructions. A putative coding sequence was isolated in a 50-μL PCR, which contained 1 μL of cDNA, 4 μL of deoxyribonucleotide triphosphates (2.5 mM each), 2 units of Ex Taq polymerase (Takara), 5 μL of 10× Ex Taq buffer, and 1 μL of specific primers (5 μM each). To isolate apyrase homologs from *P. euphratica*, we searched for a conserved domain in the plant apyrase coding sequence in public databases, including the National Center of Biotechnology Information (NCBI), Plant Transcript Assemblies (The Institute for Genomic Research), and PoplusDB. We based primer design on the coding sequence of a homologous apyrase gene from *Populus trichocarpa* (NCBI accession no. XM_002325360); the primer sequences were 5′-ATGAAACGACCTGGTTTGCGAC-3′ and 5′-TTATGCTGGTGATGACACAGCCTC-3′. The amplified cDNA product was cloned into the pMD18-T vector (Takara) for sequencing.

We amplified the mRNA transcription product of the *PeAPY2* gene (1,829 bp) with RACE (3′ RACE) and genome walking at the 5′ ends. To obtain the 3′ flanking sequence, we performed the 3′ RACE method to amplify 3′ untranslated regions, according to a lock-docking oligo(dT) primer method (Borson et al., 1992). In brief, total RNA was isolated, and reverse transcription was carried out with a lock-docking oligo$(dT)_{16}$ primer (Supplemental Table S1). Two gene-specific primers (3race-ap1 and 3race-ap2) were designed for two rounds of PCR and paired with two adaptor primers (3race-adaptor1 and 3race-adaptor2, respectively). The amplified product was cloned into the pMD18-T vector and sequenced. To obtain the 5′ flanking sequence, we performed modified thermal asymmetric interlaced (TAIL)-PCR, as described by Liu and Chen (2007). Each of four relatively long, arbitrary degenerate (LAD) primers (LAD1-1 to LAD1-4; Supplemental Table S1) was mixed with a gene-specific primer (GS-ap0) and genomic DNA in each reaction. The resulting amplified genomic fragments were diluted and used as templates in two sequential, independent, TAIL-PCRs, where an adapter primer (AC1) was paired with gene-specific nested primers, GS-ap1 and GS-ap2. The products of these two TAIL-PCRs were gel extracted and sequenced. The results showed a stop codon (TAA) within the 5′ untranslated region, which was in frame with the coding sequence. Thus, we identified the full-length *PeAPY2* coding sequence.

Sequence and Phylogenetic Analyses

Full-length amino acid sequences of apyrases from different species were identified in a BLAST search (accession numbers are shown in Supplemental Table S2) on the NCBI Web site (http://www.ncbi.nlm.nih.gov/). A multiple amino acid sequence alignment was performed with ClustalW. Signal peptide prediction was performed with the SignalP 4.0 online server (http://www.cbs.dtu.dk/services/SignalP/). Transmembrane domain analysis was performed with the TMHMM server version 2.0 (http://www.cbs.dtu.dk/services/TMHMM/). The full-length coding sequence of *PeAPY2* was 1,404 bp; this sequence encoded a putative protein of 466 amino acids (Supplemental Fig. S2) with a putative mass of 51 kD. Hydropathic analysis predicted a transmembrane domain at the N terminus of PeAPY2 (Supplemental Fig. S2). However, the SignalP program did not predict a significant signal peptide in PeAPY2. PeAPY2 contained five intact apyrase-conserved regions, five conserved regions, and three nucleotide-binding domains in the N terminus. All the conserved regions and nucleotide-binding domains could be found in orthologous apyrases from other species, including PtAPY, GhAPY1, AtAPY1, AtAPY2, RcAPY, and GS52 (Supplemental Fig. S2).

We performed a phylogenetic analysis with the neighbor-joining method in MEGA version 5.0 software (bootstrap analysis with 1,000 replicates). Neighbor-joining and parsimony trees showed similar patterns. We found that PeAPY2 was highly similar to the apyrase in *P. trichocarpa*. Moreover, PeAPY2 was closely related to the orthologous apyrase in *Ricinus communis*, cotton (*Gossypium hirsutum*), and Arabidopsis (*Arabidopsis thaliana*). However, PeAPY2 was distinct from legume-specific apyrases in *Medicago truncatula*, like GS50 and GS52 (Supplemental Fig. S3).

Subcellular Localization Analysis

We amplified the coding region of *PeAPY2* without the stop codon with the primers 5′-CACCATGAAACGACCTGGTTTGCGAC-3′ and 5′-GTGCTGGTGATGACACAGCCTC-3′. We cloned the product into the pENTR vector with the directional TOPO cloning kit (Invitrogen). After sequencing, the cDNA was directionally inserted into its destination vector, p2GWY7, with a lambda recombinase protocol (Karimi et al., 2005). This construct yielded a *PeAPY2-eYFP* fusion sequence. For the particle bombardment experiment,

strips of onion (*Allium cepa*) epidermis were placed on an MS plate supplemented with 0.8% (w/v) agar. The fusion construct and a control eYFP vector were introduced by particle bombardment with the Biolistic Particle Delivery System-1000/He (Bio-Rad). The delivery conditions were as follows: gold particle diameter, 1 μm; helium pressure, 1.07×10^4 kPa; bombardment distance, 9 cm; and chamber vacuum pressure, 88 kPa. The bombarded cells were incubated overnight on the MS solid medium at pH 6.5, due to eYFP sensitivity to acid conditions. Epidermal cells were incubated at room temperature in the dark for 15 to 20 h. YFP fluorescence was examined with a Leica SP5 confocal microscope (Leica Microsystems). Plasmolysis was induced by hyperosmotic shock with a 500 mM NaCl solution.

In vivo organelle markers were used to confirm the subcellular localization of PeAPY2 in Arabidopsis (Nelson et al., 2007). eYFP-tagged *PeAPY2* was cotransformed into Arabidopsis mesophyll protoplasts with CFP-tagged organelle markers that specifically targeted the ER (ABRC stock no. CD3-953), the Golgi network (ABRC stock no. CD3-961), or the PM (ABRC stock no. CD3-1001). These organelle markers were constructed by fusing the N terminus of the CFP sequence to well-known target proteins, including the full-length AtPIP2A, which targeted the PM; a combination of the Arabidopsis WALL-ASSOCIATED KINASE2 signal peptide and the ER retention signal, HDEL, which targeted the ER; and the soybean (*Glycine max*) α-1,2-MANNOSIDASE I peptide, which targeted the Golgi apparatus. Then, we used standard transfection protocols described by Yoo et al. (2007) with some modifications. Leaf protoplasts of Arabidopsis were isolated as described by Yoo et al. (2007). In brief, 1-mm leaf strips from 3- to 4-week-old Arabidopsis plants were digested for 2 to 4 h in enzyme solution containing 1.5% (w/v) cellulase R10 and 0.4% (w/v) macerozyme R10. After washing three times with W5 solution (2 mM MES, pH 5.7, 154 mM NaCl, 125 mM $CaCl_2$, and 5 mM KCl), protoplasts (5×10^5) were resuspended in 100 μL of protoplast solution (400 mM mannitol, 15 mM $MgCl_2$, 4 mM morpholinoethane sulfonic acid, and KOH to achieve pH 5.7). Then, we added 5 to 10 μg of each plasmid DNA. Next, we added 110 μL of transfection solution (4% [w/v] polyethylene glycol 4000, 200 mM mannitol, and 100 mM $CaCl_2$) to the previous mixture and incubated for 30 min at 23°C. Then, W5 solution (450 μL) was added to terminate the reaction, and protoplasts were resuspended in 1 mL of fresh W5. After incubating at 23°C for 12 to 16 h, fluorescent protein was visualized with a Leica SP5 confocal microscope. The excitation wavelengths were 453 nm (CFP) and 514 nm (eYFP), and the emission wavelengths were 460 to 480 nm (CFP) and 525 to 545 nm (eYFP). Confocal microscopy images were obtained using the xyz mode, which allows one to scan the *xy* plane along the *z* axis. Representative images were selected to show the targeted cell compartments, such as the PM, ER, and Golgi apparatus.

Recombinant Protein Expression and Purification

PeAPY2 harbors a hydrophobic N-terminal transmembrane domain, but it is not posttranslationally modified in the prokaryotic expression system. We found that a recombinant, full-length PeAPY2 fused to GST was insoluble; it was expressed wholly in the inclusion body of bacteria and showed little enzymatic activity, even under refolding conditions. Therefore, we removed the 59-amino acid transmembrane domain, fused it with a GST tag, and expressed the truncated PeAPY2 enzyme in *Escherichia coli*. This truncated protein was purified under native conditions for the enzymatic studies. Previous studies have shown that the transmembrane domain is not required for enzymatic activity (Wang et al., 1998; Hsieh et al., 2000). Moreover, the bacterial recombinant ectoapyrases of soybean (GS52; Tanaka et al., 2011), pea (*Pisum sativum*), and Arabidopsis exhibited enzymatic activity (Steinebrunner et al., 2000; Kawahara et al., 2003).

The vector that carried the sequence for the truncated PeAPY2 protein fused with GST (PeAPY2-GST) was constructed by first amplifying *PeAPY2* with the following primers: 5′-CCGGAATTCCGGGATTCGAGGAGTTATGC-3′ and 5′-ACGCGTCGACTTATGCTGGTGATGACAC-3′. These primers harbored *Eco*RI and *Sal*I restriction sites (underlined) to facilitate subcloning. After subcloning into the pMD18-T vector, the *PeAPY2*-GST cassette was digested and inserted into a linearized pGEX-4T-1 vector (GE Healthcare) for transformation into *E. coli* strain BL21 (DE3). Positive *E. coli* clones were selected for expression and grown in Luria-Bertani broth at 37°C until the optical density at 600 nm reached 0.5. Then, the cells were precooled to 15°C for induction. Isopropylthio-β-galactoside was added at a final concentration of 0.3 mM, and the cells were shaken overnight in the dark at 15°C to prevent excessive protein expression and misfolding. The cells were harvested by centrifugation at 6,000*g* for 10 min; then, cells were resuspended in Tris buffer (140 mM NaCl, 2.7 mM KCl, and 10 mM Tris-Cl, pH 7.3) and lysed with mild sonication. The PeAPY2-GST protein was purified with a glutathione-Sepharose 4B column (GE Healthcare) according to the manufacturer's instructions. Tris-Cl was used as a buffering agent instead of phosphate to eliminate contamination in subsequent Pi determination assays. The expressed protein was confirmed with 10% (w/v) SDS-PAGE.

Apyrase Activity Assay

Three series of experiments were conducted to characterize PeAPY2 apyrase in terms of substrate specificity, inhibitor sensitivity, and cation cofactor preference.

In the first series, PeAPY2 substrate specificity was tested with a variety of triphosphate or diphosphate nucleotides (Tanaka et al., 2011). Nucleotide hydrolysis activity was determined by measuring the release of Pi (Taussky and Shorr, 1953). The reaction solution (100 μL) contained 30 mM HEPES (pH 6.6), 3 mM $MgCl_2$, 3 mM $CaCl_2$, and 3 mM of the corresponding substrate, ATP, ADP, AMP, GTP, UTP, or CTP. The ATP-hydrolyzing activity of PeAPY2 was examined over a range of pH 6 to 8, in addition to the assays of maximal activity for hydrolyzing ATP and affinity (apparent K_m) for ATP (Tanaka et al., 2011).

In the second series, we tested PeAPY2 sensitivity to specific inhibitors of P-, V-, and F-type ATPases. The ATPase inhibitors were applied at different concentrations: NaF (fluoride inhibits pyrophosphatase) was applied at 10, 20, and 40 mM; NaN_3 (N_3 inhibits F-type ATPases) was applied at 1, 5, and 10 mM; $NaNO_3$ (NO_3 inhibits V-type ATPases) was applied at 50 mM; Na_3VO_4 (VO_4 inhibits P-type ATPases) was applied at 1 mM; $NaMoO_4$ (molybdate inhibits acid phosphatase) was applied at 1 mM; and NGXT191, which inhibits Arabidopsis and potato (*Solanum tuberosum*) apyrases, was applied at 5 μg mL^{-1}.

In the third series, we tested potential PeAPY2 cofactors for apyrase ATP hydrolysis activity by adding various divalent ions. The reaction buffer contained either a divalent metal ion (3 mM), such as Mg^{2+}, Ca^{2+}, Zn^{2+}, Cd^{2+}, Mn^{2+}, Co^{2+}, Cu^{2+}, or Ni^{2+}, or a combination of Mg^{2+} and Ca^{2+} (1.5 mM Mg^{2+} + 1.5 mM Ca^{2+}). A chelator of Mg^{2+} and Ca^{2+} (3 mM EDTA) was applied to confirm that the divalent cations (Mg^{2+} and Ca^{2+}) had enhanced PeAPY2 apyrase activity.

All the above reactions were initiated by suspending the purified PeAPY2-GST fusion protein in the buffer, then adding the test components. All reactions were processed at 37°C for 30 min and terminated with the addition of an equal volume of 10% (v/v) TCA and then chilling on ice. Ferrous sulfate-ammonium molybdate reagent (50 μL) was added to each sample, as described by Taussky and Shorr (1953). The absorption at 660 nm was measured, and Pi content was calculated based on phosphorus standards (Sigma).

Polyclonal Antibody Preparation

Polyclonal antibodies were prepared with His-tagged recombinant proteins to maintain immunogen specificity. Full-length *PeAPY2* cDNA was amplified with specific primers (5′-CCGGAATTCCGGATGAAACGACCTGGTTTGC-3′ and 5′-ACGCGTCGACTTATGCTGGTGATGACAC-3′), which harbored *Eco*RI and *Sal*I restriction sites (underlined). These products were cloned into the pET-28a vector, which carries an N-terminal His tag (Novagen). *E. coli* BL21 (DE3) cells were transformed with the recombinant plasmid, and protein expression was induced by adding 1 mM isopropylthio-β-galactoside (final concentration) and incubating for 4 h at 37°C. *E. coli* cells were then harvested and resuspended in phosphate-buffered saline. After sonication, inclusion bodies were collected by centrifugation at 12,000*g* for 15 min and washed twice with washing buffer (140 mM NaCl, 2.7 mM KCl, 10 mM Na_2HPO_4, 2 mM KH_2PO_4, and 1 M urea, pH 7.4). The inclusion bodies were then dissolved in solution buffer (140 mM NaCl, 2.7 mM KCl, 10 mM Na_2HPO_4, 2 mM KH_2PO_4, and 8 M urea, pH 7.4) and separated with SDS-PAGE. The gel was washed and stained with precooled 0.25 M KCl solution for 5 min. The distinct band that contained recombinant protein was recovered and used for rabbit immunization (CWBIO). Polyclonal antibodies were purified with the Agarose Protein A kit (CWBIO).

PeAPY2 Transformation of Arabidopsis

The full-length coding region of *PeAPY2* was cloned into a Gateway binary expression vector, pK7WG2D (Karimi et al., 2002), which contained the 35S promoter of *Cauliflower mosaic virus*. This vector was introduced into *Agrobacterium tumefaciens*, strain GV3101, and then transformed into wild-type Arabidopsis Columbia-0 with the floral dip method (Clough and Bent, 1998). pK7WG2D-GUS was a vector control, constructed and transformed in parallel with pK7WG2D-PeAPY2. Putative transgenic lines were selected with 50 mg L^{-1} kanamycin on one-half-strength MS medium that contained

1% (w/v) Suc and 0.8% (w/v) agar. Six single-copy transgenic lines of *35S::PeAPY2* and three homozygous GUS control lines from the third generation were selected according to the segregation ratio (Han et al., 2013). In our study, seedlings of wild-type, vector control, and transgenic Arabidopsis plants were grown in nursery soil under a long-day photoperiod (16 h of light and 8 h of dark) at 100 μmol m^{-2} s^{-1}, and the temperature was 22°C with 50% to 70% relative humidity.

Phenotypic Analysis of *PeAPY2*-Transgenic Plants

Wild-type, vector control, and *PeAPY2*-transgenic lines were germinated and grown on one-half-strength MS medium containing 1% (w/v) Suc and 0.8% (w/v) agar. The standard procedures for the freezing tolerance assay were carried out as described (Chinnusamy et al., 2003; Yang et al., 2010), with minor modifications. Briefly, 7-d-old seedlings of these lines were cold acclimated at 4°C for 7 d and removed to a programmed freezing chamber. The temperature in the chamber was programmed to decline at the rate of 1°C h^{-1}. Plants were maintained at −1°C for 6 h, and then the temperature was lowered to −6°C at a rate of 1°C h^{-1}. The temperature was lowered step by step (22°C → 4°C → −1°C → −6°C) to reduce the formation of ice crystals during rapid freezing, as the size of the crystals decreases with the rate of freezing (Scarth, 1944). In this study, to avoid the rapid formation of ice and mechanical injury caused by ice crystallization, cold-acclimated plants were used for freezing temperatures (Scarth, 1944). After exposure to −6°C for 2 h, plants were removed and placed at 4°C in the dark for 12 h and then transferred to light at 22°C. The temperature was gradually elevated (−6°C → 4°C → 22°C) to avoid rapid deplasmolysis and rupture of the protoplast caused by a rapid thawing (Scarth, 1944). After 3 d of recovery at 22°C, seedlings were sampled to measure relative electrolyte leakage. Separate groups of control wild-type, vector control, and transgenic lines were cultured under normal growth conditions at 22°C throughout the experiment. We estimated membrane injury in control and cold-stressed plants by measuring relative electrolyte leakage in an assay described by Uemura et al. (1995). The survival rate of wild-type, vector control, and transgenic lines was examined after 10 d of recovery.

For root growth measurements, 7-d-old plants were grown on one-half-strength MS medium and stressed at 4°C under continuous light of 100 μmol m^{-2} s^{-1}. Control plants were grown at 22°C in the same light condition. Root length was measured with image-analysis software, ImageJ (http://rsb.info.nih.gov/ij/). Primary root lengths of control and cold-stressed plants were measured to calculate the relative root length.

Cell Viability and Membrane Integrity Analyses

Seven-day-old wild-type and *PeAPY2*-transgenic lines were cold acclimated at 4°C for 7 d, transferred to −1°C for 12 h, and then moved to 4°C for 12 h. Membrane integrity was measured by double staining seedlings with FDA and FM4-64 (Invitrogen) to measure PM permeability. The confocal parameters were set as described in previous studies (Schapire et al., 2008): the excitation wavelength was 488 nm (FDA and FM4-64), and the emission wavelengths were 505 to 525 nm (FDA) and 610 to 700 nm (FM4-64).

To measure the response to eATP, 7-d-old seedlings of wild-type and transgenic lines were treated with ATP-Na_2 (800 μM) or ATPγS (800 μM) for 12 h. The pH was adjusted to 5.7 to 5.8 when ATP was applied. Then, roots were stained with FDA and PI to examine root cell viability (Cruz-Ramírez et al., 2004; Sun et al., 2012a).

We also investigated whether ATP and the apyrase products (e.g. ADP and AMP) conferred cold tolerance. Roots of wild-type and transgenic seedlings (7 d old) were incubated in a one-half-strength MS + MES (5 mM) nutrient buffer containing 0, 50, or 600 μM ATP, ADP, AMP, or PO_4^{3-} (note that an equal molar value of $CaCl_2$ was applied for the ATP treatment) for 24 h. pH was adjusted to 5.7 to 5.8 when ATP was added into the nutrient buffer. These seedlings of wild-type and transgenic lines were cold acclimated at 4°C for 1 d and subjected to low-temperature treatment: −1°C for 16 h, then the temperature was lowered to −6°C for 2 h and finally recovered at 4°C for 12 h. Roots were then stained with FDA and PI to examine root cell viability as described above.

qRT-PCR

The levels of *PeAPY2* and *PeAPY1* transcription were evaluated in cold-stressed *P. euphratica* cells with qRT-PCR. *P. euphratica* cells were placed at 4°C for cold stress, and control cells were cultured at 25°C, in the dark. Control and cold-stressed calluses were sampled at 0, 1, 5, 8, 11, 24, 48, 72, and 148 h to measure *PeAPY2* expression. Control and cold-stressed calluses were sampled at 0, 12, 24, 48, 72, and 168 h to measure *PeAPY1* expression. Callus samples were rapidly frozen in liquid nitrogen. Then, total RNA was isolated with TRIzol reagent (Invitrogen). DNA was eliminated by treating for 0.5 h with DNase I (Promega). Next, 1 μg of purified RNA was used as a template for first-strand cDNA synthesis with Moloney murine leukemia virus reverse transcriptase (Promega) and oligo(dT) primers. Specific primers were designed for *PeAPY2* and *PeAPY1* (Supplemental Table S3). Amplification was performed as described by Ding et al. (2010): 95°C for 5 min; followed by 32 cycles of 94°C for 30 s, 55°C for 30 s, and 72°C for 30 s; with a final step of 72°C for 10 min. The expression levels of target genes were normalized to the expression level of *PeACT7* using the method as described in Livak and Schmittgen (2001). Each experiment was replicated at least three times, and mean values were calculated.

To clarify whether *PeAPY2* overexpression interfered with the expression of endogenous apyrase in Arabidopsis, we examined the transcription of *AtAPY1*, *AtAPY2*, *AtAPY3*, *AtAPY4*, *AtAPY5*, *AtAPY6*, and *AtAPY7* in wild-type, vector control, and *PeAPY2*-transgenic Arabidopsis cells under normal growth conditions (22°C). Specific primers were designed for *AtAPY1* to *AtAPY7* genes (Supplemental Table S3). Total RNA was isolated from Arabidopsis seedlings, and qRT-PCR was performed as described above. The expression of the housekeeping gene, *ACTIN2*, was measured in Arabidopsis and used as the internal control (Yamazaki et al., 2008).

Measurement of Extracellular ATP

Third-generation seedlings from wild-type and *PeAPY2*-transgenic lines were germinated on one-half-strength MS medium and grown on 24-pore plates (six seedlings for each pore). Double-distilled water (100 μL) was added to each pore to maintain humidity. Before the initiation of cold treatment, 300 μL of double-distilled water was added to each pore and allowed to equilibrate for 20 min. The seedlings were transferred to a cold chamber at 4°C for 7 d, and the eATP in roots was sampled after 0, 12, 24, 48, and 96 h of cold stress. After 7 d of cold treatment, the temperature was cooled to −1°C and maintained at that temperature for 12 h. Seedlings were then transferred to 4°C for 12 h and, finally, recovery at 22°C. The liquid medium was sampled after 12 h of recovery, and samples were immediately frozen in liquid nitrogen. The eATP levels in Arabidopsis seedlings and *P. euphratica* cells were determined with the Enlighten ATP Assay System Bioluminescence Kit (Promega) as described by Sun et al. (2012b).

FM4-64 Staining for Vesicle Trafficking Assay in Arabidopsis Roots

We used a lipophilic styryl dye, FM4-64, to visualize endocytosis and vesicular trafficking. Three series of experiments were performed to clarify the effects of apyrase inhibitors, low temperature, and eATP on vesicular trafficking in Arabidopsis roots. A brief description of each series is given below.

Series 1: Apyrase Inhibitors and BFA Treatment

Roots of 7-d-old wild-type and transgenic Arabidopsis seedlings were equilibrated with liquid one-half-strength MS solution (1% [w/v] Suc, pH 5.7) for 30 min. For inhibitor treatment, roots of Arabidopsis seedlings were pretreated with NGXT191 or polyclonal antibodies against PeAPY2 for 1.5 h prior to FM4-64 staining. In brief, wild-type roots were treated with 3 μg mL^{-1} NGXT191, and the *PeAPY2*-transgenic lines were incubated with polyclonal antibodies at a ratio of 1:500 at room temperature. Untreated controls received the same concentration of the solvent dimethyl sulfoxide and preimmune serum. Thereafter, treated and untreated seedlings were stained with FM4-64 (5 μM) for 10 min, followed by washing for 15 or 30 min. To determine whether NGXT191 could suppress PeAPY2 in vivo, *PeAPY2*-transgenic lines were subjected to 0, 1.5, 3, or 6 μg mL^{-1} for 1.5 h followed by FM4-64 staining. The uptake of FM4-64 was calculated as the ratio of intracellular fluorescence to whole-cell fluorescence (Bandmann and Homann, 2012), and values were standardized to the wild-type control treated without NGXT191 (Kitakura et al., 2011).

Wild-type and transgenic plants were examined for differences in exocytosis with BFA. BFA blocks trafficking from endosomes to PM, causes the formation of endosomal aggregates (BFA compartment), and causes the redistribution of Golgi proteins to the ER (Geldner et al., 2003). Seedlings stained with FM4-64 (5 μM) were exposed to BFA (50 μM) for 1.5 h. Then, BFA was washed out for 1.5 h. FM4-64 internalization was visualized with a confocal microscope before and after BFA washing. Additionally, BFA has been variously described as an

inhibitor of endocytosis (Baluška et al., 2002; Geldner, 2004) and used to dissect trafficking pathways between different endomembrane compartments in plant cells (Geldner et al., 2003; Grebe et al., 2003; Kleine-Vehn et al., 2008). To test whether BFA inhibits endocytosis, the effects of BFA and NAA (an inhibitor of endocytosis; Paciorek et al., 2005) on vesicle trafficking were compared. Wild-type and *PeAPY2*-transgenic seedlings were exposed to BFA (10 μM) or NAA (10 μM) for 30 min, followed by FM4-64 (5 μM) staining. Then, the fluorescent dye was washed out for 30 min. FM4-64 internalization was visualized with a confocal microscope before and after BFA and NAA washing.

Series 2: Low-Temperature Treatment

Seven-day-old wild-type and transgenic seedlings were exposed to 22°C (control) or 4°C (cold stress) for 24 h prior to FM4-64 staining. Vesicular trafficking was also analyzed in cold-stressed plants during the recovery process. Cold-acclimated seedlings (4°C for 7 d) were subjected to −1°C for 6 h, then transferred to 4°C for 12 h, and finally recovered at 22°C for 24 h before FM4-64 staining. Roots were stained with FM4-64 for 10 min and washed for 30 min to remove excess dye prior to confocal analysis. Next, the seedlings were subjected to BFA (50 μM) treatment for 1.5 h. FM4-64 internalization was visualized with a confocal microscope before and after BFA washing.

Series 3: ATP and Its Metabolic Products Treatment

Roots of 7-d-old wild-type and transgenic seedlings were exposed to 0, 50, 500, or 1,000 μM ATP-Na_2 for 1.5 h or to 500 μM ATPγS for 1.5 h. Then, roots were stained with FM4-64 for 10 min and washed for 30 min prior to confocal microscopy. In addition, the effects of the products of apyrase action (i.e. ADP and AMP) were examined in root cells of wild-type and *PeAPY2*-transgenic lines. Roots of wild-type and transgenic seedlings (7 d old) were exposed to one-half-strength MS + MES (5 mM) nutrient buffer containing 0, 20, 50, 500, or 1,000 μM PO_4^{3-}, ADP, AMP, or ATP for 1.5 h. Thereafter, roots were stained with FM4-64 and used for confocal microscopy as described above. In these studies, equal molar values of $CaCl_2$ were applied for the ATP treatment and the pH was adjusted to 5.7 to 5.8 when ATP was added into the nutrient buffer.

Data Analysis

All mean data were subjected to SPSS (SPSS Statistics 17.0) for statistical tests and analyses. Unless stated otherwise, differences were considered significant at $P < 0.05$.

Supplemental Data

The following supplemental materials are available.

Supplemental Figure S1. Expression profiles of *PeAPY1* in *P. euphratica* callus cells under cold stress.

Supplemental Figure S2. Multiple sequence alignment of PeAPY2 (apyrase from *P. euphratica*) with other apyrases from different species.

Supplemental Figure S3. Phylogenetic relationships between PeAPY2 and other representative APY proteins from different plant species.

Supplemental Figure S4. The ATP-hydrolyzing activity of PeAPY2 and the affinity for ATP.

Supplemental Figure S5. Effects of pH and ATPase inhibitors on PeAPY2 apyrase activity.

Supplemental Figure S6. Expression profiles of *AtAPY1*, *AtAPY2*, *AtAPY3*, *AtAPY4*, *AtAPY5*, *AtAPY6*, and *AtAPY7* in wild-type, vector control, and *PeAPY2*-transgenic Arabidopsis.

Supplemental Figure S7. Effects of NGXT191 on vesicular trafficking in root cells of wild-type and *PeAPY2*-transgenic lines.

Supplemental Figure S8. Effects of NAA and BFA on vesicular trafficking in root cells of wild-type and *PeAPY2*-transgenic lines.

Supplemental Figure S9. Effects of ATP and the apyrase products on cell viability in wild-type and *PeAPY2*-transgenic lines under control and cold stress conditions.

Supplemental Figure S10. Effects of ATPγS on cell viability in wild-type and *PeAPY2*-transgenic lines.

Supplemental Figure S11. Effects of ATP and the apyrase products on vesicular trafficking in wild-type and *PeAPY2*-transgenic lines.

Supplemental Table S1. Primers used for gene cloning of *P. euphratica PeAPY2*.

Supplemental Table S2. Accession numbers of apyrase orthologs used in multiple sequence alignment and phylogenetic analysis.

Supplemental Table S3. Primer sets used for qRT-PCR.

ACKNOWLEDGMENTS

We thank the Functional Genomics Unit, Plant Systems Biology (Flanders Interuniversity Institute of Biotechnology, Ghent University), for providing the Gateway destination vectors; Dr. Yong-Fu Fu and Dr. Xu Wang (Chinese Academy of Agricultural Sciences) for providing multiple CFP-tagged organelle markers; Dr. Stanley J. Roux (University of Texas) for kindly providing the apyrase inhibitor NGXT191; Dr. Meiqin Liu (Beijing Forestry University) for assistance in the operation of the confocal microscope; and the Platform of Large Instruments and Equipment at Beijing Forestry University for allowing the use of the confocal microscope.

Received April 20, 2015; accepted July 28, 2015; published July 29, 2015.

LITERATURE CITED

Abeijon C, Yanagisawa K, Mandon EC, Häusler A, Moremen K, Hirschberg CB, Robbins PW (1993) Guanosine diphosphatase is required for protein and sphingolipid glycosylation in the Golgi lumen of *Saccharomyces cerevisiae*. J Cell Biol **122:** 307–323

Baluška F, Hlavačka A, Šamaj J, Palme K, Robinson DG, Matoh T, McCurdy DW, Menzel D, Volkmann D (2002) F-actin-dependent endocytosis of cell wall pectins in meristematic root cells: insights from brefeldin A-induced compartments. Plant Physiol **130:** 422–431

Bandmann V, Homann U (2012) Clathrin-independent endocytosis contributes to uptake of glucose into BY-2 protoplasts. Plant J **70:** 578–584

Bolte S, Talbot C, Boutte Y, Catrice O, Read ND, Satiat-Jeunemaitre B (2004) FM-dyes as experimental probes for dissecting vesicle trafficking in living plant cells. J Microsc **214:** 159–173

Borson ND, Salo WL, Drewes LR (1992) A lock-docking oligo(dT) primer for 5′ and 3′ RACE PCR. PCR Methods Appl **2:** 144–148

Cannon SB, McCombie WR, Sato S, Tabata S, Denny R, Palmer L, Katari M, Young ND, Stacey G (2003) Evolution and microsynteny of the apyrase gene family in three legume genomes. Mol Genet Genomics **270:** 347–361

Cao Y, Tanaka K, Nguyen CT, Stacey G (2014) Extracellular ATP is a central signaling molecule in plant stress responses. Curr Opin Plant Biol **20:** 82–87

Chinnusamy V, Ohta M, Kanrar S, Lee BH, Hong X, Agarwal M, Zhu JK (2003) ICE1: a regulator of cold-induced transcriptome and freezing tolerance in *Arabidopsis*. Genes Dev **17:** 1043–1054

Chiu TY, Christiansen K, Moreno I, Lao J, Loqué D, Orellana A, Heazlewood JL, Clark G, Roux SJ (2012) AtAPY1 and AtAPY2 function as Golgi-localized nucleoside diphosphatases in *Arabidopsis thaliana*. Plant Cell Physiol **53:** 1913–1925

Chivasa S, Murphy AM, Hamilton JM, Lindsey K, Carr JP, Slabas AR (2009) Extracellular ATP is a regulator of pathogen defence in plants. Plant J **60:** 436–448

Clark G, Fraley D, Steinebrunner I, Cervantes A, Onyirimba J, Liu A, Torres J, Tang W, Kim J, Roux SJ (2011) Extracellular nucleotides and apyrases regulate stomatal aperture in Arabidopsis. Plant Physiol **156:** 1740–1753

Clark G, Roux SJ (2009) Extracellular nucleotides: ancient signaling molecules. Plant Sci **177:** 239–244

Clark G, Roux SJ (2011) Apyrases, extracellular ATP and the regulation of growth. Curr Opin Plant Biol **14:** 700–706

Clark G, Torres J, Finlayson S, Guan X, Handley C, Lee J, Kays JE, Chen ZJ, Roux SJ (2010a) Apyrase (nucleoside triphosphate-diphosphohydrolase) and extracellular nucleotides regulate cotton fiber elongation in cultured ovules. Plant Physiol **152:** 1073–1083

Clark G, Wu M, Wat N, Onyirimba J, Pham T, Herz N, Ogoti J, Gomez D, Canales AA, Aranda G, et al (2010b) Both the stimulation and inhibition of root hair growth induced by extracellular nucleotides in Arabidopsis

are mediated by nitric oxide and reactive oxygen species. Plant Mol Biol **74:** 423–435

Clark GB, Morgan RO, Fernandez MP, Salmi ML, Roux SJ (2014) Breakthroughs spotlighting roles for extracellular nucleotides and apyrases in stress responses and growth and development. Plant Sci **225:** 107–116

Clough SJ, Bent AF (1998) Floral dip: a simplified method for *Agrobacterium*-mediated transformation of *Arabidopsis thaliana*. Plant J **16:** 735–743

Cruz-Ramírez A, López-Bucio J, Ramírez-Pimentel G, Zurita-Silva A, Sánchez-Calderon L, Ramírez-Chávez E, González-Ortega E, Herrera-Estrella L (2004) The xipotl mutant of *Arabidopsis* reveals a critical role for phospholipid metabolism in root system development and epidermal cell integrity. Plant Cell **16:** 2020–2034

Day RB, McAlvin CB, Loh JT, Denny RL, Wood TC, Young ND, Stacey G (2000) Differential expression of two soybean apyrases, one of which is an early nodulin. Mol Plant Microbe Interact **13:** 1053–1070

Demidchik V, Shang Z, Shin R, Colaço R, Laohavisit A, Shabala S, Davies JM (2011) Receptor-like activity evoked by extracellular ADP in Arabidopsis root epidermal plasma membrane. Plant Physiol **156:** 1375–1385

Ding M, Hou P, Shen X, Wang M, Deng S, Sun J, Xiao F, Wang R, Zhou X, Lu C, et al (2010) Salt-induced expression of genes related to Na^+/K^+ and ROS homeostasis in leaves of salt-resistant and salt-sensitive poplar species. Plant Mol Biol **73:** 251–269

Emans N, Zimmermann S, Fischer R (2002) Uptake of a fluorescent marker in plant cells is sensitive to brefeldin A and wortmannin. Plant Cell **14:** 71–86

Etzler ME, Kalsi G, Ewing NN, Roberts NJ, Day RB, Murphy JB (1999) A nod factor binding lectin with apyrase activity from legume roots. Proc Natl Acad Sci USA **96:** 5856–5861

Feraru E, Feraru MI, Asaoka R, Paciorek T, De Rycke R, Tanaka H, Nakano A, Friml J (2012) BEX5/RabA1b regulates trans-Golgi network-to-plasma membrane protein trafficking in *Arabidopsis*. Plant Cell **24:** 3074–3086

Fujii T, Minagawa T, Shimizu T, Takeguchi N, Sakai H (2012) Inhibition of ecto-ATPase activity by curcumin in hepatocellular carcinoma HepG2 cells. J Physiol Sci **62:** 53–58

Gao XD, Kaigorodov V, Jigami Y (1999) *YND1*, a homologue of *GDA1*, encodes membrane-bound apyrase required for Golgi *N*- and *O*-glycosylation in *Saccharomyces cerevisiae*. J Biol Chem **274:** 21450–21456

Geldner N (2004) The plant endosomal system: its structure and role in signal transduction and plant development. Planta **219:** 547–560

Geldner N, Anders N, Wolters H, Keicher J, Kornberger W, Muller P, Delbarre A, Ueda T, Nakano A, Jürgens G (2003) The *Arabidopsis* GNOM ARF-GEF mediates endosomal recycling, auxin transport, and auxin-dependent plant growth. Cell **112:** 219–230

Gerasimenko JV, Gerasimenko OV, Petersen OH (2001) Membrane repair: Ca^{2+}-elicited lysosomal exocytosis. Curr Biol **11:** R971–R974

Grebe M, Xu J, Möbius W, Ueda T, Nakano A, Geuze HJ, Rook MB, Scheres B (2003) *Arabidopsis* sterol endocytosis involves actin-mediated trafficking via ARA6-positive early endosomes. Curr Biol **13:** 1378–1387

Han Y, Wang W, Sun J, Ding M, Zhao R, Deng S, Wang F, Hu Y, Wang Y, Lu Y, et al (2013) *Populus euphratica* XTH overexpression enhances salinity tolerance by the development of leaf succulence in transgenic tobacco plants. J Exp Bot **64:** 4225–4238

Hsieh HL, Song CJ, Roux SJ (2000) Regulation of a recombinant pea nuclear apyrase by calmodulin and casein kinase II. Biochim Biophys Acta **1494:** 248–255

Idone V, Tam C, Goss JW, Toomre D, Pypaert M, Andrews NW (2008) Repair of injured plasma membrane by rapid Ca^{2+}-dependent endocytosis. J Cell Biol **180:** 905–914

Jeter CR, Tang W, Henaff E, Butterfield T, Roux SJ (2004) Evidence of a novel cell signaling role for extracellular adenosine triphosphates and diphosphates in *Arabidopsis*. Plant Cell **16:** 2652–2664

Karimi M, De Meyer B, Hilson P (2005) Modular cloning in plant cells. Trends Plant Sci **10:** 103–105

Karimi M, Inzé D, Depicker A (2002) Gateway vectors for *Agrobacterium*-mediated plant transformation. Trends Plant Sci **7:** 193–195

Kawahara T, Toyoda K, Kiba A, Miura A, Ohgawara T, Yamamoto M, Inagaki Y, Ichinose Y, Shiraishi T (2003) Cloning and characterization of pea apyrases: involvement of PsAPY1 in response to signal molecules from the pea pathogen *Mycosphaerella pinodes*. J Gen Plant Pathol **69:** 33–38

Kim SH, Yang SH, Kim TJ, Han JS, Suh JW (2009) Hypertonic stress increased extracellular ATP levels and the expression of stress-responsive genes in *Arabidopsis thaliana* seedlings. Biosci Biotechnol Biochem **73:** 1252–1256

Kim SY, Sivaguru M, Stacey G (2006) Extracellular ATP in plants: visualization, localization, and analysis of physiological significance in growth and signaling. Plant Physiol **142:** 984–992

Kitakura S, Vanneste S, Robert S, Löfke C, Teichmann T, Tanaka H, Friml J (2011) Clathrin mediates endocytosis and polar distribution of PIN auxin transporters in *Arabidopsis*. Plant Cell **23:** 1920–1931

Kleine-Vehn J, Dhonukshe P, Sauer M, Brewer PB, Wiśniewska J, Paciorek T, Benková E, Friml J (2008) ARF GEF-dependent transcytosis and polar delivery of PIN auxin carriers in *Arabidopsis*. Curr Biol **18:** 526–531

Knowles AF (2011) The GDA1_CD39 superfamily: NTPDases with diverse functions. Purinergic Signal **7:** 21–45

Lam SK, Cai Y, Tse YC, Wang J, Law AH, Pimpl P, Chan HY, Xia J, Jiang L (2009) BFA-induced compartments from the Golgi apparatus and trans-Golgi network/early endosome are distinct in plant cells. Plant J **60:** 865–881

Lim MH, Wu J, Yao J, Gallardo IF, Dugger JW, Webb LJ, Huang J, Salmi ML, Song J, Clark G, et al (2014) Apyrase suppression raises extracellular ATP levels and induces gene expression and cell wall changes characteristic of stress responses. Plant Physiol **164:** 2054–2067

Liu X, Wu J, Clark G, Lundy S, Lim M, Arnold D, Chan J, Tang W, Muday GK, Gardner G, et al (2012) Role for apyrases in polar auxin transport in Arabidopsis. Plant Physiol **160:** 1985–1995

Liu YG, Chen Y (2007) High-efficiency thermal asymmetric interlaced PCR for amplification of unknown flanking sequences. Biotechniques **43:** 649–650, 652, 654

Livak KJ, Schmittgen TD (2001) Analysis of relative gene expression data using real-time quantitative PCR and the $2^{-\Delta\Delta CT}$ method. Methods **25:** 402–408

Los FC, Kao CY, Smitham J, McDonald KL, Ha C, Peixoto CA, Aroian RV (2011) RAB-5- and RAB-11-dependent vesicle-trafficking pathways are required for plasma membrane repair after attack by bacterial pore-forming toxin. Cell Host Microbe **9:** 147–157

Marcus AJ, Broekman MJ, Drosopoulos JH, Islam N, Pinsky DJ, Sesti C, Levi R (2003) Metabolic control of excessive extracellular nucleotide accumulation by CD39/ecto-nucleotidase-1: implications for ischemic vascular diseases. J Pharmacol Exp Ther **305:** 9–16

Massalski C, Bloch J, Zebisch M, Steinebrunner I (2015) The biochemical properties of the Arabidopsis ecto-nucleoside triphosphate diphosphohydrolase AtAPY1 contradict a direct role in purinergic signaling. PLoS ONE **10:** e0115832

McNeil PL (2002) Repairing a torn cell surface: make way, lysosomes to the rescue. J Cell Sci **115:** 873–879

McNeil PL, Miyake K, Vogel SS (2003) The endomembrane requirement for cell surface repair. Proc Natl Acad Sci USA **100:** 4592–4597

Nelson BK, Cai X, Nebenführ A (2007) A multicolored set of *in vivo* organelle markers for co-localization studies in Arabidopsis and other plants. Plant J **51:** 1126–1136

Okuhata R, Otsuka Y, Tsuchiya T, Kanzawa N (2013) Mutagenesis of apyrase conserved region 1 alters the nucleotide substrate specificity. Plant Signal Behav **8:** e24131

Okuhata R, Takishima T, Nishimura N, Ueda S, Tsuchiya T, Kanzawa N (2011) Purification and biochemical characterization of a novel ecto-apyrase, MP67, from *Mimosa pudica*. Plant Physiol **157:** 464–475

Paciorek T, Zazímalová E, Ruthardt N, Petrásek J, Stierhof YD, Kleine-Vehn J, Morris DA, Emans N, Jürgens G, Geldner N, et al (2005) Auxin inhibits endocytosis and promotes its own efflux from cells. Nature **435:** 1251–1256

Reddy A, Caler EV, Andrews NW (2001) Plasma membrane repair is mediated by Ca^{2+}-regulated exocytosis of lysosomes. Cell **106:** 157–169

Riewe D, Grosman L, Fernie AR, Wucke C, Geigenberger P (2008) The potato-specific apyrase is apoplastically localized and has influence on gene expression, growth, and development. Plant Physiol **147:** 1092–1109

Roux SJ, Song C, Jeter C (2006) Regulation of plant growth and development by extracellular nucleotides. *In* F Baluška, S Mancuso, D Volkmann, eds,

Communication in Plants: Neuronal Aspects of Plant Life. Springer, Berlin, pp 221–234

Roux SJ, Steinebrunner I (2007) Extracellular ATP: an unexpected role as a signaler in plants. Trends Plant Sci **12:** 522–527

Scarth GW (1944) Cell physiological studies of frost resistance: a review. New Phytol **43:** 1–12

Schapire AL, Valpuesta V, Botella MA (2009) Plasma membrane repair in plants. Trends Plant Sci **14:** 645–652

Schapire AL, Voigt B, Jasik J, Rosado A, Lopez-Cobollo R, Menzel D, Salinas J, Mancuso S, Valpuesta V, Baluska F, et al (2008) *Arabidopsis* synaptotagmin 1 is required for the maintenance of plasma membrane integrity and cell viability. Plant Cell **20:** 3374–3388

Schiller M, Massalski C, Kurth T, Steinebrunner I (2012) The Arabidopsis apyrase AtAPY1 is localized in the Golgi instead of the extracellular space. BMC Plant Biol **12:** 123

Shibasaki K, Uemura M, Tsurumi S, Rahman A (2009) Auxin response in *Arabidopsis* under cold stress: underlying molecular mechanisms. Plant Cell **21:** 3823–3838

Song CJ, Steinebrunner I, Wang X, Stout SC, Roux SJ (2006) Extracellular ATP induces the accumulation of superoxide via NADPH oxidases in Arabidopsis. Plant Physiol **140:** 1222–1232

Sonnemann KJ, Bement WM (2011) Wound repair: toward understanding and integration of single-cell and multicellular wound responses. Annu Rev Cell Dev Biol **27:** 237–263

Steinebrunner I, Jeter C, Song C, Roux SJ (2000) Molecular and biochemical comparison of two different apyrases from *Arabidopsis thaliana*. Plant Physiol Biochem **38:** 913–922

Steinebrunner I, Wu J, Sun Y, Corbett A, Roux SJ (2003) Disruption of apyrases inhibits pollen germination in Arabidopsis. Plant Physiol **131:** 1638–1647

Sun J, Zhang CL, Deng SR, Lu CF, Shen X, Zhou XY, Zheng XJ, Hu ZM, Chen SL (2012a) An ATP signalling pathway in plant cells: extracellular ATP triggers programmed cell death in *Populus euphratica*. Plant Cell Environ **35:** 893–916

Sun J, Zhang X, Deng S, Zhang C, Wang M, Ding M, Zhao R, Shen X, Zhou X, Lu C, et al (2012b) Extracellular ATP signaling is mediated by H_2O_2 and cytosolic Ca^{2+} in the salt response of *Populus euphratica* cells. PLoS ONE **7:** e53136

Takahashi H, Toyoda K, Hirakawa Y, Morishita K, Kato T, Inagaki Y, Ichinose Y, Shiraishi T (2006) Localization and responsiveness of a cowpea apyrase VsNTPase1 to phytopathogenic microorganisms. J Gen Plant Pathol **72:** 143–151

Tam C, Idone V, Devlin C, Fernandes MC, Flannery A, He X, Schuchman E, Tabas I, Andrews NW (2010) Exocytosis of acid sphingomyelinase by wounded cells promotes endocytosis and plasma membrane repair. J Cell Biol **189:** 1027–1038

Tanaka K, Gilroy S, Jones AM, Stacey G (2010) Extracellular ATP signaling in plants. Trends Cell Biol **20:** 601–608

Tanaka K, Nguyen CT, Libault M, Cheng J, Stacey G (2011) Enzymatic activity of the soybean ecto-apyrase GS52 is essential for stimulation of nodulation. Plant Physiol **155:** 1988–1998

Taussky HH, Shorr E (1953) A microcolorimetric method for the determination of inorganic phosphorus. J Biol Chem **202:** 675–685

Todorov LD, Mihaylova-Todorova S, Westfall TD, Sneddon P, Kennedy C, Bjur RA, Westfall DP (1997) Neuronal release of soluble nucleotidases and their role in neurotransmitter inactivation. Nature **387:** 76–79

Togo T, Alderton JM, Bi GQ, Steinhardt RA (1999) The mechanism of facilitated cell membrane resealing. J Cell Sci **112:** 719–731

Togo T, Krasieva TB, Steinhardt RA (2000) A decrease in membrane tension precedes successful cell-membrane repair. Mol Biol Cell **11:** 4339–4346

Uemura M, Joseph RA, Steponkus PL (1995) Cold acclimation of *Arabidopsis thaliana*: effect on plasma membrane lipid composition and freeze-induced lesions. Plant Physiol **109:** 15–30

Vanegas D, Clark G, Cannon AE, Roux S, Chaturvedi P, McLamore ES (2015) A self-referencing biosensor for real-time monitoring of physiological ATP transport in plant systems. Biosens Bioelectron **74:** 37–44

Wang Q, Kong L, Hao H, Wang X, Lin J, Samaj J, Baluska F (2005) Effects of brefeldin A on pollen germination and tube growth: antagonistic effects on endocytosis and secretion. Plant Physiol **139:** 1692–1703

Wang R, Chen S, Deng L, Fritz E, Hüttermann A, Polle A (2007) Leaf photosynthesis, fluorescence response to salinity and the relevance to chloroplast salt compartmentation and anti-oxidative stress in two poplars. Trees (Berl) **21:** 581–591

Wang R, Chen S, Zhou X, Shen X, Deng L, Zhu H, Shao J, Shi Y, Dai S, Fritz E, et al (2008) Ionic homeostasis and reactive oxygen species control in leaves and xylem sap of two poplars subjected to NaCl stress. Tree Physiol **28:** 947–957

Wang TF, Guidotti G (1996) CD39 is an ecto-(Ca^{2+},Mg^{2+})-apyrase. J Biol Chem **271:** 9898–9901

Wang TF, Ou Y, Guidotti G (1998) The transmembrane domains of ectoapyrase (CD39) affect its enzymatic activity and quaternary structure. J Biol Chem **273:** 24814–24821

Webb MS, Steponkus PL (1993) Freeze-induced membrane ultrastructural alterations in rye (*Secale cereale*) leaves. Plant Physiol **101:** 955–963

Weerasinghe RR, Swanson SJ, Okada SF, Garrett MB, Kim SY, Stacey G, Boucher RC, Gilroy S, Jones AM (2009) Touch induces ATP release in Arabidopsis roots that is modulated by the heterotrimeric G-protein complex. FEBS Lett **583:** 2521–2526

Wei QJ (1993) Euphratica Poplar (in Chinese). Chinese Forestry Press, Beijing

Windsor B, Roux SJ, Lloyd A (2003) Multiherbicide tolerance conferred by AtPgp1 and apyrase overexpression in *Arabidopsis thaliana*. Nat Biotechnol **21:** 428–433

Wu J, Steinebrunner I, Sun Y, Butterfield T, Torres J, Arnold D, Gonzalez A, Jacob F, Reichler S, Roux SJ (2007) Apyrases (nucleoside triphosphate-diphosphohydrolases) play a key role in growth control in Arabidopsis. Plant Physiol **144:** 961–975

Yamaguchi-Shinozaki K, Shinozaki K (2006) Transcriptional regulatory networks in cellular responses and tolerance to dehydration and cold stresses. Annu Rev Plant Biol **57:** 781–803

Yamazaki T, Kawamura Y, Minami A, Uemura M (2008) Calcium-dependent freezing tolerance in *Arabidopsis* involves membrane resealing via synaptotagmin SYT1. Plant Cell **20:** 3389–3404

Yamazaki T, Takata N, Uemura M, Kawamura Y (2010) *Arabidopsis* synaptotagmin SYT1, a type I signal-anchor protein, requires tandem C2 domains for delivery to the plasma membrane. J Biol Chem **285:** 23165–23176

Yang H, Shi Y, Liu J, Guo L, Zhang X, Yang S (2010) A mutant CHS3 protein with TIR-NB-LRR-LIM domains modulates growth, cell death and freezing tolerance in a temperature-dependent manner in *Arabidopsis*. Plant J **63:** 283–296

Yoo SD, Cho YH, Sheen J (2007) *Arabidopsis* mesophyll protoplasts: a versatile cell system for transient gene expression analysis. Nat Protoc **2:** 1565–1572

Zonia L, Munnik T (2008) Vesicle trafficking dynamics and visualization of zones of exocytosis and endocytosis in tobacco pollen tubes. J Exp Bot **59:** 861–873